Science of the Total Environment 791 (2021) 148101

Contents lists available at ScienceDirect

Science of the Total Environment

journal homepage: www.elsevier.com/locate/scitotenv

Investigating the potential of Sentinel-2 configuration to predict the quality of Mediterranean permanent grasslands in open woodlands

Jesús Fernández-Habas [a], Alma María García Moreno [a], Mª. Teresa Hidalgo-Fernández [a], José Ramón Leal-Murillo [a], Begoña Abellanas Oar [a], Pedro J. Gómez-Giráldez [b], María P. González-Dugo [b], Pilar Fernández-Rebollo [a,*]

[a] Department of Forest Engineering, ETSIAM, University of Cordoba, Ctra. Madrid, Km 396, 14071 Córdoba, Spain
[b] IFAPA, Institute of Agricultural and Fisheries Research and Training of Andalusia, Avd. Menéndez Pidal s/n, 14071 Cordoba, Spain

HIGHLIGHTS

- Sentinel-2 allowed qualitative assessment of CP and NDF in Mediterranean grassland.
- Red-edge band and SWIR region showed highest contribution to predict CP and NDF.
- Field spectroscopy and Sentinel-2 data can be combined for larger model dataset.

GRAPHICAL ABSTRACT

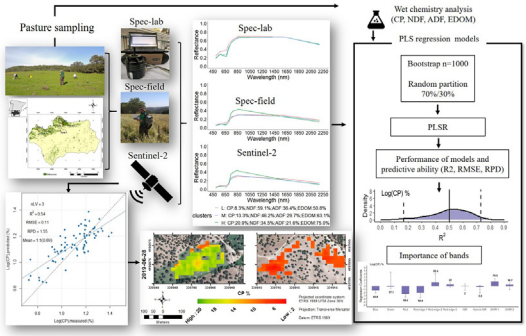

ARTICLE INFO

Article history:
Received 18 February 2021
Received in revised form 24 May 2021
Accepted 24 May 2021
Available online 29 May 2021

Editor: Paulo Pereira

Keywords:
Crude protein
fibre
digestibility
Dehesa management
PLS
canopy reflectance

ABSTRACT

The assessment of pasture quality in permanent grasslands is essential for their conservation and management, as it can contribute to making real-time decisions for livestock management. In this study, we assessed the potential of Sentinel-2 configuration to predict forage quality in high diverse Mediterranean permanent grasslands of open woodlands. We evaluated the performance of Partial Least Squares Regression (PLS) models to predict crude protein (CP), neutral detergent fibre (NDF), acid detergent fibre (ADF) and enzyme digestibility of organic matter (EDOM) by using three different reflectance datasets: (i) laboratory measurements of reflectance of dry and ground pasture samples re-sampled to Sentinel-2 configuration (Spec-lab) (ii) field in-situ measurements of grasslands canopy reflectance resampled to Sentinel-2 configuration (Spec-field); (iii) and Bottom Of Atmosphere Sentinel-2 imagery. For the three reflectance datasets, the models to predict CP content showed moderate performance and predictive ability. Mean $R^2_{test} = 0.68$ were obtained using Spec-lab data, mean R^2_{test} decreased by 0.11 with Spec-field and by 0.18 when Sentinel-2 reflectance was used. Statistics for NDF showed worse predictions than those obtained for CP: predictions produced with Spec-lab showed mean $R^2_{test} = 0.64$ and mean $RPD_{test} = 1.73$. The mean values of $R^2_{test} = 0.50$ and $RPD_{test} = 1.54$ using Sentinel-2 BOA reflectance were marginally better than the values obtained with Spec-field (mean $R^2_{test} = 0.48$, mean $RPD_{test} = 1.43$). For ADF and EDOM, only predictions made with Spec-lab produced acceptable results. Bands from the red-edge region, especially band 5, and the SWIR regions showed the highest contribution to estimating CP and NDF. Bands 2, blue and 4, red also seem to be important. The implementation of field spectroscopy in combination with Sentinel-2 imagery proved to be feasible to produce forage quality maps and to develop larger datasets. This study contributes to increasing knowledge of the potential and applicability of Sentinel-2 to predict the quality of Mediterranean permanent grasslands in open woodlands.

* Corresponding author.
E-mail address: ir1ferep@uco.es (P. Fernández-Rebollo).

https://doi.org/10.1016/j.scitotenv.2021.148101

1. Introduction

Mediterranean permanent grasslands are present in South Africa, California, Chile, southern Australia and in the Mediterranean basin itself (Cosentino et al., 2014), being the latter a global biodiversity hotspot due to its high number of endemic plants (Myers et al., 2000). Mediterranean grasslands play a vital role to satisfy the demand for animal products and the provision of ecosystem services such as carbon sequestration, control of soil erosion and wildfires, and biodiversity conservation (Porqueddu et al., 2016; Porqueddu et al., 2017). Permanent grasslands in the Mediterranean basin are especially important in open woodland, which cover about 3.1 million hectares in Spain and Portugal (Moreno and Pulido, 2009). This savanna-like agroforestry system, known as *Dehesa* in Spain and *Montado* in Portugal is recognised as a highly biodiverse and multifunctional ecosystem, being an example of the integration of land-use and biodiversity conservation (Bugalho et al., 2011; Moreno and Pulido, 2009; Plieninger and Wlbrand, 2001). *Dehesa* and *Montado* farms are devoted to livestock rearing at low stocking rates whose feed relies mainly on rain-fed permanent grasslands and acorn of evergreen oaks (Plieninger and Wlbrand, 2001).

These grasslands are species-rich communities with high diversity and mainly dominated by annuals (Marañón, 1991; Olea and San Miguel-Ayanz, 2006) with a low yield that is strongly affected by the inter- and intra- annual variability of rainfall (Cosentino et al., 2014; Olea and San Miguel-Ayanz, 2006). Its high diversity together with the low synchrony among species and functional groups (Pérez-Ramos et al., 2020) contribute to increasing the spatial and temporal heterogeneity in pasture production and quality of these grasslands. Under future climate change conditions, the expected reduction of rainfall and the uncertainty on its inter-annual distribution (Giannakopoulos et al., 2009; Giorgi and Lionello, 2008) challenges the productivity of Mediterranean grasslands and hence, their capacity to sustain livestock production and their associated ecosystem services (Ma et al., 2017). In this context, the development of tools for continuous monitoring to provide real-time information for decision-making has become pivotal for the conservation and efficient management of permanent grasslands (Defourny et al., 2019; Gómez-Giráldez et al., 2019; Stumpf et al., 2020; Wolfert et al., 2017). The use of remote-sensing technologies is proving to be a promising tool to support efficient management of permanent grasslands through the provision of information about botanical composition, structure, phenology, quantity and quality (Ali et al., 2016; Fauvel et al., 2020; Gómez-Giráldez et al., 2020; Wachendorf et al., 2018). Quality can be defined as the set of properties inherent to grasslands that allow assessing their value. In this study, we refer to the quality of grasslands as their value to feed livestock. In this context, grasslands quality depends on properties such as nutrients concentration and physical composition that determine the intake, digestibility and partitioning of metabolized products (Dumont et al., 2015). Pasture quality is estimated by chemical analyses that typically report the content of crude protein or nitrogen, ash, fibre (acid detergent fibre and neutral detergent fibre), metabolisable energy and digestibility (Dumont et al., 2015; Pullanagari et al., 2013). There are other parameters relevant to livestock performance such as biomass. In this study, we will focus on quality, determined by the following pasture quality variables: crude protein (CP), neutral detergent fibre (NDF), acid detergent fibre (ADF) and enzyme digestibility of organic matter (EDOM). Based on this definition of pasture quality and the variables studied, a pasture of high quality is characterised by a high content of CP and a low content of fibres which leads to a high EDOM. Assessment of pasture quality is essential for the management of grasslands as it is crucial to make real-time decisions for adjusting stocking rates, carrying capacity and additional feedstuff needs (Raab et al., 2020; Ramoelo and Cho, 2018; Starks et al., 2006). Laboratory chemical methods have been traditionally used to determine the quality of grasslands. Conversely to remote-sensing techniques, laboratory methods are costly, time-consuming and do not provide real-time information or possibilities for grassland quality mapping (Mansour et al., 2012; Starks et al., 2006). The amount of destructive sampling required to obtain representative data, the difficulty to access some sampling sites and the delay between sampling and availability of the results determine the low practicability of laboratory-based methods to assess pasture quality in Mediterranean grasslands (Pullanagari et al., 2013). Remote-sensing-based methods allow timely spatial predictions at a lower cost with the disadvantage of a lowered accuracy of the assessments (Pullanagari et al., 2013). However, the commented advantages might compensate the loss of accuracy and facilitate its implementation in farms of Mediterranean open woodlands. The development in the last decades of new remote-sensing technologies such as unmanned aerial vehicles (UAVs) equipped with hyperspectral cameras and machine learning algorithms enable more accurate predictions of grassland quality (Ali et al., 2016; Gao, 2006). UAVs can provide hyperspectral data at high spatial resolution; however, this technology needs to be operated by specialised companies, which might imply an economic constraint (Askari et al., 2019; Raab et al., 2020). In order to facilitate the applicability to farm management, the technology to implement must be low-cost and easy to use by farmers and grassland managers. Satellite images, although at a coarser resolution, can provide information for evaluating large areas. The Sentinel-2 satellite constellation, launched in 2015, has proven to be a promising tool for permanent grassland monitoring (Punalekar et al., 2018). Sentinel-2 is a sensor system developed by the European Space Agency (ESA) that provide freely available data worldwide with a revisiting time of 5 days and 13 spectral bands: four bands at 10 m, six bands at 20 m and three bands at 60 m spatial resolution (ESA, 2020). The spectral configuration of Sentinel-2, with the availability of three red-edge and two NIR bands has a great potential to study grassland quality due to the known sensibility of these regions of the spectrum to changes in nitrogen, chlorophyll and fibre content of plants (Curran et al., 1992; Frampton et al., 2013; Jacquemoud et al., 1995; Kawamura et al., 2008; Kokaly, 2001). It allows establishing relationships between reflectance at certain Sentinel-2 bands with grassland quality parameters CP, NDF, ADF and digestibility. In the last decades new algorithms of multivariate machine learning have arisen and gained popularity such as of Partial Least Squares Regression (PLS), random forest, support vector machine and artificial neural network. In particular, PLS has become the state-of-the-art method and one the most widespread and efficient techniques to analyse spectroscopy data (Kucheryavskiy, 2018; Wold et al., 2001). In addition to be one of the most studied and robust methods to deal with reflectance and forage data, its popularity is also due to the few hyperparameters that need to be set; only the number of latent variables (PLS components) used to decompose the predictors and responses which can be determined by automatically cross-validation (Kucheryavskiy, 2018).

Previous studies have aimed at establishing relationships between Sentinel-2 bands and grassland quality parameters. Ramoelo et al. (2015) demonstrated the potential of Sentinel-2 to predict leaf nitrogen content in rangelands from South Africa using simulated Sentinel-2 data, reporting R^2 values of 0.90 with high importance of the red-edge and shortwave region bands. Raab et al. (2020) investigated the use of Sentinel-1 and Sentinel-2 data to estimate pasture quantity and quality of semi-natural grasslands in the south-east of Germany and obtained high R^2 values for ADF concentration ($R^2 = 0.79$) and CP ($R^2 = 0.72$) with the bands from the narrow near-infrared and red-edge regions being the most important ones for the predictions. The utility of combining resampled field spectra data and actual satellite images to predict grass foliar nitrogen concentration, CP and NDF have also been explored in previous studies (Lugassi et al., 2019; Mutanga et al., 2015; Ramoelo and Cho, 2018). In some of these works, field spectroscopy has allowed the development of models based on spectroradiometer data resampled to Sentinel-2 configuration that can be used on Sentinel-2 images (Ramoelo and Cho, 2018). The comparison of models for pasture quality estimation using spectral data resampled to Sentinel-2 spectral

configuration recorded with both, field spectroradiometers on grassland canopy and with Visible-Near-Infrared (Vis-NIRS) spectrometer on dried and ground pasture samples, can provide useful information. For example, they can inform about the potential of Sentinel-2 to predict pasture quality in high diverse Mediterranean permanent grasslands and be used to investigate the factors affecting the accuracy of models. In particular, field spectroscopy can contribute to developing more robust models. Some of the limiting factors to calibrate robust models with Sentinel-2 data are the labour of intensive sampling collection, the match between the sampled data and the reflectance at pixel level in heterogeneous grasslands, and the mismatch between sampling and Sentinel-2 data (Pullanagari et al., 2013; Ramoelo and Cho, 2018). Field spectroscopy data can be easily collected ensuring a good match between the sampled data and the reflectance recorded. It is more flexible in terms of collecting a wide range of data due to the finer spatial resolution (Pullanagari et al., 2012; Pullanagari et al., 2021). Also, it can help to overcome the constrain of scattered trees in open woodlands to obtain tree-free signal of reflectance to calibrate predictive models. Therefore, the combination of field spectroscopy resampled to Sentinel-2 spectral configuration and Sentinel-2 imagery can be an interesting approach to facilitate the use of Sentinel-2 in the management of grasslands from open woodlands.

Overall, there is a need for information about the potential of Setinel-2 for the management and conservation of high diverse permanent Mediterranean grasslands and the limitations affecting its implementation. The availability of high-quality pasture for grazing livestock has been pointed out as essential by stakeholders of agroforestry systems to ensure the system resilience (Camilli et al., 2018). Extensive systems such as *Dehesa*, rely mainly on pasture to feed the livestock (Olea and San Miguel-Ayanz, 2006). Therefore, it is of key importance for farmers of open woodlands grasslands to have timely information about the pasture quality. Through targeted management, remote sensing of pasture quality using Sentinel-2 data can contribute to a more efficient and competitive management of open woodlands farms. In the context of conservation, *Dehesa* and *Montados* are considered as habitats to be protected under the European Habitats Directive ("Dehesas with evergreen Quercus spp", code 6310) (Habitats Directive, 1992), which means that the member states are obligated to guarantee the good state of conservation of this habitat. Its conservation relies on the land use by grazing livestock in a human-managed extensive system and can therefore be altered by both overgrazing and abandonment (Moreno and Pulido, 2009). This association between conservation and land use has motivated its acknowledgement as a typical high nature value (HNV) farmland area (Paracchini et al., 2008; Ferraz-de-Oliveira et al., 2016). The continuous monitoring of the pasture quality of these systems using remote sensing can be implemented to facilitate a management compatible with the conservation of this high-interest ecosystem.

There are very few studies focused on monitoring pasture quality in high diverse permanent Mediterranean grasslands using remotely sensed data (Lugassi et al., 2019; Serrano et al., 2018). In this study, the potential and limitations of Sentinel-2 configuration to promote and facilitate the implementation of this technology in Mediterranean permanent grasslands is investigated. In particular, we evaluate the accuracy PLS models to predict CP, NDF, ADF and EDOM in high diverse Mediterranean permanent grasslands based on data from: (i) laboratory measurements of Vis-NIRS reflectance of dry and ground pasture samples resampled to Sentinel-2 configuration (ii) field in-situ measurements of grassland canopy reflectance resampled to Sentinel-2 configuration; (iii) and Bottom Of Atmosphere Sentinel-2 imagery. The contribution of specific Sentinel-2 bands to these predictions and the combination of satellite imagery with field spectroscopy for pasture quality estimation and mapping was also explored. This study will provide further insight into the potential of Sentinel-2 configuration to estimate pasture quality with PLS models and the implications and limitations of this technology for the management of Mediterranean permanent grasslands of open woodlands.

2. Material and methods

2.1. Study area

The study was carried out on eight *Dehesa* farms from the southern Spain region of Andalusia (Fig. 1). This region is characterised by a Mediterranean continental climate with hot summers and cool rainy winters. Soils are mainly cambisols, with pH ~5–7, with a loamy-clay and loamy-sandy texture and low fertility (CSIC-IARA, 1989). The general topography is flat or characterised by a sequence of rolling hills and plateaus, with no pronounced slopes. The altitude ranges from 370 m.a.s.l. to 750 m.a.s.l. The mean annual rainfall varies from 516 mm to 620 mm along the farms and the mean annual temperature is around 17 °C (Global Climate Monitor, 2020). Two of the farms are devoted to sheep and Iberian pig breeding and the other six to cattle and Iberian pig breeding. Permanent grasslands of farms included plant communities dominated by annual low-grown herbs and grasses belonging to the *Helianthemetalia guttati, Malcomietalia* and *Poetalia bulbosae* alliances (Rodwell et al., 2002). Irrigated grasslands of *Trifolium repens* and *Lolium* spp. and permanent grasslands reseeded with commercial seed mixtures, mainly legumes, were also present on these farms.

2.2. Grassland sampling and reference measurements

Grassland samplings were conducted during the growing season of 2012–2013 in farms 1–4 and during the growing season of 2018–2019 in farms 5–8. These samplings were designed to cover the different types of grasslands of *Dehesa* farms throughout the growing season. It included permanent natural grasslands, reseeded grasslands with commercial seed mixes and irrigated grasslands. The pasture sampling carried out in 2012–2013 was designed to study the effect of grazing on pasture quality (Fernández et al., 2014). For that purpose, one grazing exclusion plot of 4×8 m was established per farm in permanent natural grasslands from farms 1 to 4. Samples of pasture contained in sampling quadrats (0.4×0.4 m) were cut to ground level, four inside and four outside of the exclusion plots. Eight samples were collected per farm (farms 1 to 4) in five dates, January/February, March, April, May and June, which provided with 160 samples. After removing 35 samples from quadrats with extremely low pasture production or partially covering bare ground, 125 were available from the 2012–2013 sampling campaign. The design of the sampling campaign of 2018–2019 was governed by the presence of adjacent trees, which together with the geolocation error of 10 m 95.45% conf. level of Sentinel-2 (Gascon et al., 2017) may affect the reflectance of proximal pixels. 25 tree-free 20×20 m Sentinel-2 pixels were identified in total on fields of the farms 5 to 8 (13 in permanent natural grasslands, 9 in reseeded grassland and 3 in irrigated grasslands). Once located the pixels on the ground using a SXBlue II GPS sub-meter receiver (Geneq inc, Montreal, Quebec, Canada) we selected one the 10×10 m pixel, from now on referred to as "site", and we randomly set four sampling quadrats (0.4×0.4 m) and the pasture contained in it cut to ground level. This sampling was repeated on three dates: November/December, February and May (Tables 1 and S1) over the 25 pixels which provided 300 samples from 2018 to 2019. With both sampling campaigns, 425 samples were available for modelling (Table S1).

The pasture samples were dried in the oven for 48 h at 60 °C and ground to pass through a 1-mm sieve. Then, the ground samples were subjected to chemical analysis for crude protein (CP), neutral detergent fibre (NDF), acid detergent fibre (ADF) and enzyme digestibility of organic matter (EDOM) at the Laboratory of Animal Nutrition of SERIDA (Villaviciosa, Spain).

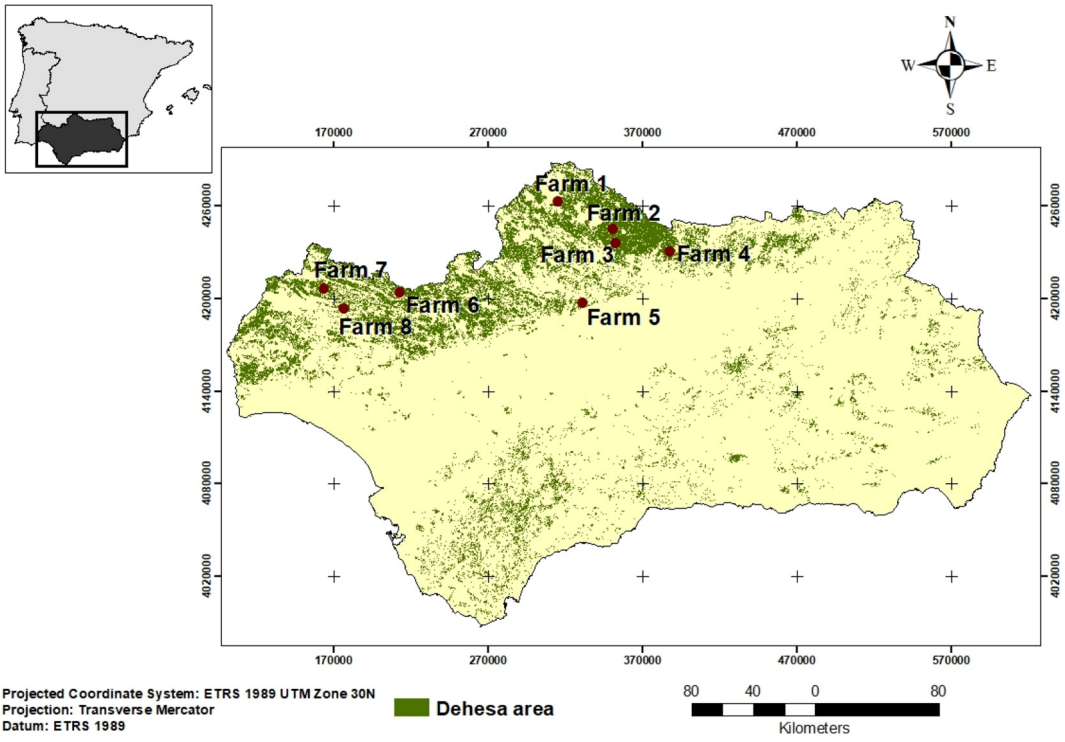

Fig. 1. Location of farms in the *Dehesa* area of Andalusia (Spain) where permanent grasslands were sampled. Source: Dehesa area illustrated in green is provided by the WMS of the Dehesa systems distribution in Andalusia (REDIAM, 2020).

2.3. Spectra measurement and processing

From the 2012–2013 sampling campaign, field in-situ canopy reflectance was available for all samples (125 samples), whereas from the second sampling campaign (2018–2019) field in-situ reflectance was measured in the sampling performed in May (48 samples) on farm 5, which adds up to 173 samples (Spec-field from now on) (Fig. 2). Spec-field reflectance spectra of the pasture contained within the sampling quadrats (0.4 × 0.4 m) was measured with an ASD FieldSpec Spectroradiometer (ASD Inc., Boulder, Colorado, USA) before cutting the pasture. Reflectance was measured in the whole range of 350 nm to 2500 nm with an interpolated resolution of 1 nm. This interpolation is done internally by the spectrometer, which has a resolution of 1.4 nm in the 350–1000 nm range (SWIR-1 sensor) and 2 nm in the 1000–2500 nm range (SWIR-2 sensor). The spectra were taken using a fibre optic probe attached to the pistol grip between 10:00 and 15:00 under clear sky conditions from a nadir orientation at 1.20 m height resulting in a 0.22 m^2 recording area. Four reflectance measurements were recorded for each sampling quadrat and white references were taken on a Spectralon panel (Labsphere, NorthSutton, NH) every four samples. The final reflectance measurement representative of each quadrant was the average of the four replicates.

For comparison purposes, the spectrum Vis-NIRS of these 173 pasture samples was recorded in a laboratory after drying and grounding the samples (Spec-lab from now on). Spec-lab measurements of the ground samples were scanned with a portable LabSpec 5000 spectrometer (ASD Inc., Boulder, Colorado, USA) using IndicoPro 6.0 spectrum acquisition software. The equipment has a nominal spectral resolution of 3 nm at 700 nm (visible and near-infrared region) and 10 nm at 1400 and 2100 nm (short-wavelength infrared region). Internal data sampling rate of spectrometer (1.4 nm at 350–1000 nm and 2.2 nm at 1001–2500 nm) is interpolated to 1 nm across the full spectral range (350–2500 nm). The pasture samples were measured using High-Intensity Muglight, model-A122100, (ASD Inc.) equipped with a sapphire window using an ASDI sampling tray adapter with a quartz window having a 110 mm^2 spot diameter (ASD Inc.). Four replicates of each sample were scanned, two for each tray adapter by rotating it 45°. An average of 50 spectra was collected from each replicate and stored as an average spectrum. White reference scans were taken between every sample scan. The final spectrum was obtained by averaging the four replicates.

Both, Spec-field and Spec-lab measurements were then spectrally resampled to match the spectral specifications of the Sentinel-2 data (Table 2). The spectral resampling was performed using the "*resample2*" function of the *prospectr* package (Stevens and Ramirez-Lopez, 2014) in R v. 3.6.1 (R Development Core Team, 2019). This function resamples the original signal to a lower resolution signal (configuration of Sentinel-2 data in this case) using full-width half maximum (FWHM) values (Stevens and Ramirez-Lopez, 2014; Lugassi et al., 2019). Band 1, band 9 and band 10 were excluded from all the analyses in this study because of their coarser spatial resolution (60 m) as their main use is atmospheric applications.

Level-2A Bottom Of Atmosphere (BOA) reflectance Sentinel-2 data (ESA, 2020) of the 25 selected pixels of 20 and 10 m resolution of

Table 1
Sentinel-2 data acquisitions and sampling date of the pasture samples.

Farm	Sampling date	Sentinel-2 data acquisitions	Spacecraft	Tile
Farm 5	2018-11-29	2018-11-30	Sentinel-2A	30SUH
	2019-02-19	2019-02-21	Sentinel-2A	
	2019-05-14	2019-05-14	Sentinel-2B	
Farm 6	2018-12-05	2018-11-28	Sentinel-2B	29SQC
	2019-02-25	2019-02-26	Sentinel-2B	
	2019-05-07	2019-05-07	Sentinel-2B	
Farm 7	2018-12-04	2018-12-06	Sentinel-2A	29SPC
	2019-02-26	2019-02-26	Sentinel-2B	
	2019-05-08	2019-05-05	Sentinel-2A	
Farm 8	2018-12-04	2018-12-08	Sentinel-2B	29SQB
	2019-02-26	2019-02-26	Sentinel-2B	
	2019-05-08	2019-05-07	Sentinel-2B	

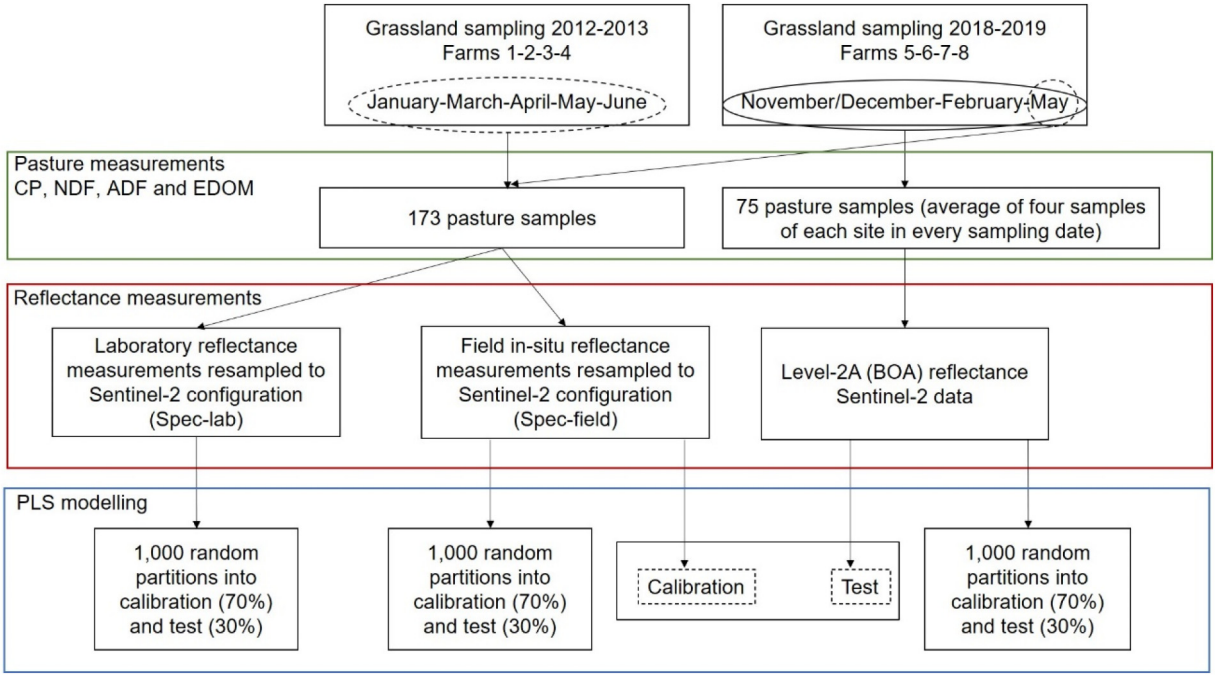

Fig. 2. Conceptual framework of the modelling approach followed in this study.

farms 5 to 8 was extracted on the three different dates (Table 1) from Google Earth Engine platform (Gorelick et al., 2017). Data was extracted ensuring that the images were cloud- and cloud shadow-free over the study area. Bands of 20 m resolution were not resampled to 10 m spatial resolution to prevent the inclusion of tree signal from adjacent pixels. Level-2A product are derived from the associated Level-1C products and are systematically generated by ESA for the Euro-Mediterranean region since March 2018 (ESA, 2020). Using Sen2Cor processor, the Level 1C input data are atmospheric-, terrain and cirrus corrected to deliver the final Level-2A products (Mueller-Wilm et al., 2017).

The differences of the three reflectance datasets and their variations related to the pasture quality variables were evaluated. All analyses of this study were performed in R v. 3.6.1 (R Development Core Team, 2019). The K-mean cluster analysis using the variables of pasture quality was performed using the *kmeans* function of the *"factoextra"* package (Kassambara and Mundt, 2017). The number of clusters was defined by the "elbow method", being three the optimal number (Kodinariya and Makwana, 2013). The average reflectance spectra of the clusters obtained was calculated and plotted for the three reflectance datasets.

Table 2
Spectral and spatial specifications of the Sentinel-2 bands.

Band	Band Centre (nm)	Bandwidth (nm)	Spatial resolution (m)
1-Coastal aerosol	443	20	60
2-Blue	490	65	10
3-Green	560	35	10
4-Red	665	30	10
5-Red-edge-1	705	15	20
6-Red-edge-2	740	15	20
7-Red-edge-3	783	20	20
8-Near-infrared (NIR)	842	115	10
8A-Narrow NIR	865	20	20
9-Water vapour	945	20	60
10-Short-wave infrared (SWIR)-cirrus	1375	30	60
11-SWIR-1	1610	90	20
12-SWIR-2	2190	180	20

2.4. Modelling approach and statistical analysis

The potential of Sentinel-2 configuration to estimate pasture quality was compared between Spec-lab, Spec-field and Sentinel-2 BOA reflectance. Since Spec-field measurements were available from the 2012–2013 sampling (125 samples) and May from 2018 to 2019 sampling on farm 5 (48 samples), the same 173 samples were available to compare Spec-lab and Spec-field-based modelling as mentioned above (Fig. 2). For Sentinel-2 BOA-based modelling, the pasture quality measurements of the four quadrats at each one of the 25 sites selected were averaged for every sampling, so a representative value of the quality variable at the site could be associated with its corresponding reflectance on each of the three dates ($N = 75$). A table summarising the grassland samplings and data used for each reflectance dataset can be found in Table S1 of Supplementary Material.

When PLS and other machine learning algorithms are used, is key to develop a representative training dataset of the spectral features of the vegetation to calibrate robust models. Outliers in the training data can lead to biased predictions and underfit of the models (Wang et al., 2018). Outliers, which can be defined as samples departing from the bulk of the data can be produced by objects belonging to underrepresented data or samples from another population, laboratory errors or instrument errors (Martens and Naes, 1992; Valderrama et al., 2007). Since these sources of errors are common in Vis-NIRS spectroscopy and remote sensing, detection of outliers is commonly applied (Morellos et al., 2016; Xu et al., 2018; Xu et al., 2014). The novel outlier detection approach based on Projection-Based Modelling implemented in *"mdatools"* was used to exclude outlier samples (Kucheryavskiy, 2019; Rodionova and Pomerantsev, 2020). This method is based on the calculation of the score distance, orthogonal distance, and Y-residuals which are used to compute a so-called "total distance" of every sample, and an outlier threshold for outlier detection in regression problems (Rodionova and Pomerantsev, 2020). The method consists of an iterative process that avoids masking and swamping effects in outlier removal. Further detailed information on the method and examples can be obtained in Rodionova and Pomerantsev (2020) and Kucheryavskiy (2020a).

Relationships between pasture quality variables (CP, NDF, ADF and EDOM) and reflectance were assessed using Partial Least Squares Regression (PLS) models performed with *"mdatools"* package (Kucheryavskiy, 2019; Kucheryavskiy, 2020b). Pasture quality measurements were log- or squared transformed when necessary to meet normality (Shapiro-Wilk test, $p > 0.05$). Although non-normally distributed data can be used to fit PLS models, substantial loss of power of PLS models was observed when small datasets were used (Goodhue et al., 2012). PLS regression is a standard and widely-used tool in chemometrics (Wold et al., 2001) and prediction of pasture quality (Lobos et al., 2013; Parrini et al., 2018). It relates a vector Y with the response variable (CP, NDF, ADF or EDOM) and a matrix X with the predictor variables (reflectance values at the Sentinel-2 bands) by a lineal multivariate regression model. PLS decomposes Y and X on *n* orthogonal latent variables (LVs) (PLS-components) that maximise the covariance between response and predictors (Wold, 1966; Zhou et al., 2019). By using these LVs, calibration equations can be created to predict the variable of interest Y, when a new X matrix is used. This method is highly effective in dealing with collinearity and a high number of predictor variables (Wold et al., 2001).

Data were randomly split into 70% for calibration and 30% for the external test. The models built with the calibration set were validated using leave-one-out (LOO) cross-validation. The optimal number of LVs was selected according to the Wold's R criterion, which is based on the cross-validation. During LOO cross-validation, N-1 models (N being the number of samples) of one LV are built by iteratively withholding each sample (one sample at a time is kept out the calibration and used for prediction). The total Predicted Error Sum of Squares (PRESS) is calculated by summing the PRESS of the N-1 models. This procedure is repeated for *n* LVs until the ratio between PRESS value of the current and the next LV is the unity (Wold, 1978; Li et al., 2002). This value denotes that the optimal number of LVs has been reached. The R^2, Root Mean Squared Error (RMSE), bias, Standard Error of Prediction (SEP) and Ratio of Predicted Deviation (RPD) were used to assess and validate the models. The R^2 is a measure of how well the data fit the regression model. The RMSE is used to assess the average accuracy of the prediction. The SEP indicates the precision of the predictions while the bias is the systematic difference between the predicted and the measured values. The RPD is the ratio of the standard deviation of the pasture quality variables from the SEP and is used to estimate the predictive ability of the model. An RPD value of one would mean that the SEP is equal to the standard deviation of the laboratory measurements and therefore, the model would have no use for predictions. Using R^2 and RPD, the prediction ability of the models can be classified following the thresholds proposed by Askari et al. (2015) and used by Askari et al. (2019) to assess PLS predictive models built with Sentinel-2 data: "excellent" (RPD ≥ 2.5 and $R^2 \geq 0.8$), "good" ($2 \leq$ RPD < 2.5 and $R^2 \geq 0.7$), "moderate" ($1.5 \leq$ RPD < 2 and $R^2 \geq 0.60$) and "poor" accuracy(RPD < 1.5 and $R^2 < 0.6$). Viscarra Rossel et al. (2006) classified RPD values as: RPD values between 1.4 and 1.8 indicate fair predictive ability, useful only for qualitative assessments and correlations while RPD values over 1.8 can be used for quantitative assessments.

The importance of the bands in the predictive models was assessed by looking at the regression coefficients of the PLS models. The inference of the regression coefficients was obtained by applying a Jack-Knifing approach implemented in *"mdatools"* package (Kucheryavskiy, 2020b). Jack-Knifing is a resampling method used to calculate bias and the variance of estimates (Martens and Martens, 2000; Friedl and Stampfer, 2002). The resamples are generated by deleting single cases from the original sample (Friedl and Stampfer, 2002). In this case, Jack-Knifing was used to calculate a *p*-value of the regression coefficients of the PLS models by setting the Jack-Knifing option and full cross-validation in *"mdatools"* (Kucheryavskiy, 2020b). A regression coefficient was considered as significant when the Jack-Knifing inferred *p*-value was <0.05.

Given the relatively small size of the datasets, the stability (or the robustness) of the models was tested by a bootstrap procedure. Following the approach of Mutanga et al. (2004) and Kawamura et al. (2008), the random partition in calibration (70%) and test (30%) was repeated 1000 times with replacement. A PLS model was built for each partition and the value of R^2, RMSE, RPD and regression coefficients were extracted. Mean and confidence intervals (CI) (2.5 and 97.5 percentiles) of R^2, RMSE, RPD and regression coefficients were reported. The number of LVs was described by the mode of the 1000 models. This procedure improves the methodology of previous studies in which a single value of these statistics is reported using a dataset of similar size (Askari et al., 2019; Lugassi et al., 2019; Ramoelo et al., 2015). The bootstrap procedure allowed determining the certainty of the results reported by each model (Mutanga et al., 2004; Mutanga et al., 2015). For the regression coefficients, the percentage of times that each band resulted as significant ($p < 0.05$, according to Jack-Knifing procedure) in the 1000 models was also included in order to assess their stability.

2.5. Spatial predictions based on Sentinel-2 imagery using models calibrated with field spectrometry

The use of field spectrometry to calibrate PLS predictive models based on Sentinel-2 configuration was investigated by "combining" the whole Spec-field dataset ($N = 173$) for calibration and cross-validation and the Sentinel-2 BOA dataset ($N = 75$) for test. Since the reflectance spectra of the two datasets were acquired using different sensors, the representativity of both sets was checked by Principal Components Analysis (PCA) based on the covariance matrix, and the Distance of Mahalanobis (DMH). These algorithms helped to evaluate that the calibration set and the test set showed representativity (they are in the same spatial space and have the same variance–covariance) so that the prediction error depended on the model, and not on the differences of the data sets (Jouan-Rimbaud et al., 1998). The reflectance values of both sets were subjected to a PCA and plotted over a score plot to check the overlap of their spatial location. Additionally, the DMHs of each Sentinel-2 sample to the centre of the population was calculated in order to identify extremely different observations of the overall characteristics of the calibration dataset (Spec-field). According to Shenk and Westerhaus (1996) criterion, sample spectra with DMH > 3.0 are not suitable to be predicted.

After the PLS model was calibrated and cross validated with the Spec-field dataset, the reflectance values of the Sentinel-2 data were used to test the predictive accuracy and precision over CP, NDF, ADF and EDOM. The R^2, RPD and RMSE of calibration, cross-validation and test of the model were reported. Spatial prediction maps at 10 m resolution over fields of irrigated and natural grasslands were computed using the calibration model and Sentinel-2 free cloud images on four different dates (2018-11-13; 2019-04-04; 2019-05-07; 2019-06-28). Pixels with tree influence on the reflectance value were excluded from the mapping. For ease of maps interpretation, CP values were back-transformed to the original scale with the follow adjustment for variance:

$$\hat{y} = 10^{\left(\widehat{\Psi} + \frac{\frac{1}{N}\sum_{i=1}^{N}\left(\widehat{\Psi}_i - \Psi_i\right)^2}{2}\right)},$$

where $\hat{y}$ are the back-transformed values, $\widehat{\Psi}$ are the estimated and Ψ the observed values, both on the logarithmic scale. The expression of the numerator in the exponent represents the mean squared error of the test dataset.

3. Results

3.1. Pasture quality values

An overview of the pasture quality values provided by the samplings is summarised in Table 3. Due to the diverse grasslands sampled and mainly to the different dates of sampling throughout the growing season, there was a large variation and wide range of values within all the pasture quality variables. CP showed a range of 24 points in the dataset used in combination with Spec-lab and Spec-field. For the same dataset, NDF showed a range of 46.5 points, while ADF reported a lower range, 29.1 points. The largest range was obtained for EDOM with a value of 47.8 points. The range of variables used for the analysis using Sentinel-2 images was lower. Overall, in both datasets, CP and EDOM values decreased from November to July while the opposite occurred with NDF and ADF (Fig. S1). CP was the variable that showed the largest variation, with a coefficient of variation of 46.2% for the dataset used for Spec-lab and Spec-field and 34.3% for the reference measurements used with Sentinel-2 BOA reflectance data. NDF and ADF showed a CV of 21% for the Spec-lab and Spec-field dataset, slightly higher than the CV of EDOM (19%). The CV of the fibres was lower in the Sentinel-2 dataset. The EDOM values used for the Sentinel-2 dataset showed the lowest variation (CV = 12%).

Fig. 3 A illustrates the groups produced by a K-means cluster analysis performed using the pasture variables. Three clusters of samples can be identified showing clear differences in their pasture quality variables. The higher the CP and EDOM % of the clusters, the lower the NDF and ADF% and vice versa. The pasture quality can be ordered from lower to higher quality as: cluster L < cluster M < cluster H. These differences between clusters can also be observed in some regions of the mean reflectance spectra of Spec-lab, Spec-field and Sentinel-2 BOA of each cluster (Fig. 3b; c; d). Spec-field and Sentinel-2 mean reflectance is very similar, showing the comparable features in the spectra. For the three sets of reflectance datasets, the clusters M and H, with higher CP and EDOM, showed lower reflectance values than the mean reflectance of the cluster L along the visible (490–665 nm) region of the spectra, especially in band 4 (red-665 nm). In the case of Spec-lab, this difference remains in the Red-edge (705–783 nm) and NIR region (Fig. 3. b). In Spec-field and Sentinel-2 datasets, the mean reflectance of cluster H was clearly higher in the Red-edge (705–783 nm) and NIR regions (842–865 nm) than the reflectance spectra of clusters L and M. Finally, the mean reflectance values of the three clusters for Spec-field and Sentinel-2 showed some differences in bands 11 and 12 (SWIR region;1610–2190 nm) while for Spec-lab reflectance, these values were identical.

3.2. Performance of models

Table 4 shows the mean, the confidence intervals of R^2, RMSE and the mode of nLV for calibrations and R^2, RMSE and RPD for cross-validations as summary of the 1000 PLS models built for each reflectance dataset (Spec-lab, Spec-field and Sentinel-2 BOA). To predict CP using Spec-lab reflectance data, the mode of LVs used to build the models was 5. For the rest of the models, the mode of LVs was 2–3 depending on the combinations of variables/reflectance data. Models fitted with Spec-lab data performed better than models based on Spec-field and Sentinel-2 BOA. Overall, means of R^2 and RPD decreased according to the reflectance data used following the order of Spec-lab>Spec-field>Sentinel-2 BOA. The opposite occurred with RMSE and the amplitude of the CI models fitted with Sentinel-2 data reported higher RMSE values and wider CI than models fitted with Spec-field and Spec-lab respectively. The statistics of models built with Spec-lab data reflect acceptable calibration models with R^2_{cv} and RPD_{cv} mean values over 0.60 and 1.60 respectively (Table 4).

Acceptable calibration models were obtained to predict CP with Spec-lab (mean R^2_{cv} = 0.69 and mean RPD_{cv} = 1.80) and Spec-field

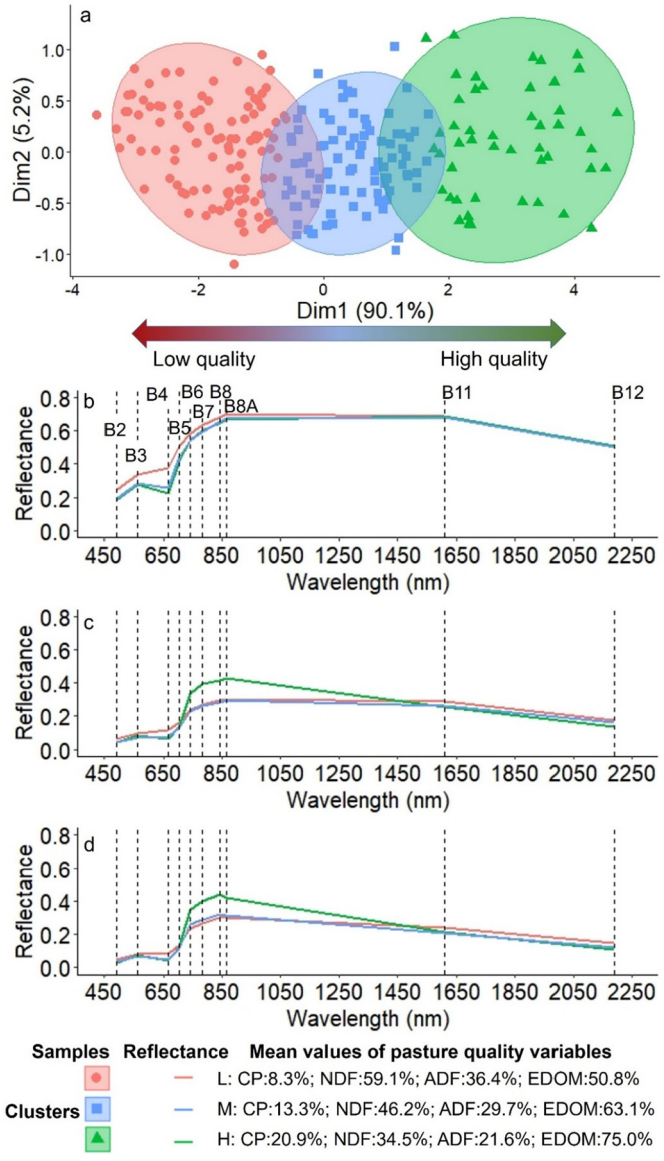

Fig. 3. (a) Results of K-means clusters analysis performed using the following pasture variables: Crude protein (CP), neutral detergent fibre (NDF), acid detergent fibre (ADF), and enzyme digestibility of organic matter (EDOM). The ellipse represents the 95% confidence interval. L, Cluster grouping low quality samples; M, Cluster grouping medium quality samples; H, Cluster grouping high quality samples. Mean reflectance of samples included in each cluster at the centre of Sentinel-2 bands for: Spec-lab dataset (N = 173) (b), Spec-field dataset (N = 173) (c) and Sentinel-2 BOA dataset (N = 75) (d).

Table 3
Descriptive statistics of the pasture quality variables used to fit the PLS models.

	Pasture variables (% DM)	Minimum	Mean	Maximum	Range	SD	CV
Spec-lab and Spec-field (N = 173)	CP	3.7	12.2	27.7	24.0	5.7	46.2
	NDF	24.9	51.2	71.3	46.5	10.7	20.9
	ADF	15.7	31.3	44.8	29.1	6.6	21.0
	EDOM	38.5	59.0	86.2	47.8	11.2	19.0
Sentinel-2 (N = 75)	CP	5.3	13.4	26.0	20.7	4.6	34.3
	NDF	31.7	45.4	69.6	37.9	8.9	19.6
	ADF	16.8	30.1	39.0	22.2	5.4	17.9
	EDOM	42.7	62.8	80.6	37.9	7.9	12.6

CP-Crude protein; NDF-neutral detergent fibre; ADF-acid detergent fibre; EDOM-enzyme digestibility of organic matter; SD- Standard deviation; CV- coefficient of variation.

Table 4
Summary statistics of calibration models for Spec-lab, Spec-field and Sentinel-2 datasets. Mean and confidence intervals (95%) of R^2, RMSE, RPD and mode of nLV calculated from N = 1000 random partitions of the datasets.

Spectral data	Variable	n	Mean	nLV	R^2 cal	RMSE cal	R^2 cv	RMSE cv	RPD cv
Spec-lab	Log (CP) %	124	1.04 [0.86]	5	0.73 (0.68–0.78)	0.10 (0.09–0.11)	0.69 (0.63–0.74)	0.11 (0.10–0.12)	1.80 (1.65–1.97)
	NDF^2g/10 g	124	27.38 [44.12]	3	0.69 (0.64–0.75)	5.81 (5.17–6.26)	0.66 (0.61–0.72)	6.11 (5.55–6.53)	1.72 (1.60–1.89)
	ADF^2g/10 g	124	10.24 [17.10]	2	0.66 (0.62–0.69)	2.31 (2.14–2.47)	0.63 (0.59–0.67)	2.39 (2.21–2.54)	1.66 (1.58–1.76)
	Log (EDOM) %	124	1.76 [0.35]	2	0.73 (0.67–0.79)	0.043 (0.037–0.047)	0.70 (0.65–0.76)	0.045 (0.040–0.049)	1.85 (1.69–2.04)
Spec-field	Log (CP) %	124	1.04 [0.86]	3	0.64 (0.58–0.70)	0.12 (0.11–0.13)	0.61 (0.54–0.67)	0.12 (0.12–0.13)	1.60 (1.48–1.74)
	NDF^2g/10 g	124	27.38 [44.12]	3	0.49 (0.41–0.58)	7.39 (6.85–7.83)	0.46 (0.37–0.55)	7.66 (7.07–8.12)	1.36 (1.27–1.49)
	ADF^2g/10 g	124	10.24 [17.10]	3	0.48 (0.41–0.57)	2.84 (2.56–3.04)	0.45 (0.37–0.54)	2.94 (2.65–3.15)	1.35 (1.27–1.47)
	Log (EDOM) %	124	1.76 [0.35]	3	0.53 (0.43–0.62)	0.056 (0.050–0.064)	0.49 (0.39–0.60)	0.058 (0.052–0.064)	1.41 (1.28–1.58)
Sentinel-2	Log (CP) %	55	1.10 [0.67]	3	0.62 (0.54–0.71)	0.10 (0.08–0.11)	0.52 (0.43–0.62)	0.11 (0.09–0.12)	1.47 (1.33–1.64)
	Log (NDF) %	55	1.65 [0.33]	3	0.61 (0.52–0.71)	0.05 (0.04–0.06)	0.53 (0.43–0.64)	0.06 (0.06–0.05)	1.48 (1.34–1.67)
	ADF^2g/10 g	55	9.38 [12.10]	2	0.40 (0.29–0.51)	2.39 (2.14–2.64)	0.33 (0.22–0.43)	2.54 (2.28–2.77)	1.23 (1.14–1.34)
	EDOM %	55	62.7 [35.2]	2	0.40 (0.25–0.55)	6.01 (4.93–6.86)	0.32 (0.19–0.44)	6.43 (5.48–7.13)	1.23 (1.12–1.35)

CP-Crude protein; NDF-neutral detergent fibre; ADF-acid detergent fibre; EDOM-enzyme digestibility of organic matter; Mean - average of pasture variable measured with range of the observed values in squared brackets; nLV- mode of the number of latent variables; RMSE- root mean square error; RPD-ratio of predicted deviation; cal- calibration statistics; cv-cross-validation statistics. Values in brackets correspond to the confidence interval (2.5 and 97.5 percentiles). A different transformation was applied to NDF and EDOM for Sentinel-2 dataset.

(mean R^2_{cv} = 0.61 and mean RPD_{cv} = 1.60). In models built with Sentinel-2 data for CP prediction, mean R^2_{cv} and mean RPD_{cv} were lower, 0.52 and 1.47 respectively, although the upper limit of CI of the 1000 models laid over 0.60 in R^2_{cv} and over 1.60 in RPD_{cv} (Table 4). Moderate results were obtained by models calibrated for NDF with Spec-lab (mean R^2_{cv} = 0.66 and mean RPD_{cv} = 1.72) and poor with Spec-field (mean R^2_{cv} = 0.46 and mean RPD_{cv} = 1.36). The statistics obtained when Sentinel-2 data was used to predict NDF (mean R^2_{cv} = 0.53 and mean RPD_{cv} = 1.48) were slightly better than in models run with Spec-field, with values of the upper limits of the CI of 0.64 in R^2_{cv} and 1.67 in RPD_{cv} indicating that some models of the 1000 runs had moderate prediction ability. The calibration model statistics obtained for ADF were very poor for models fitted with Spec-field and Sentinel-2. The best statistics were obtained for EDOM prediction models that showed a mean R^2 value of 0.70 and RPD of 1.85. However, these statistics dropped to very low values when the models were built with Spec-field and Sentinel-2 reflectance data.

Results of the predictions on the external test samples are presented in Fig. 4. (a) (Spec-lab and Spec-field) and Fig. 4. (b) (Sentinel-2). The figures show the density distribution of the 1000 values of R^2_{test}, $RMSE_{test}$ and RPD_{test} calculated by the bootstrap procedure, indicating the mean and the CI (2.5 and 97.5 percentiles). As for the calibration, the test statistics showed an overall decreasing performance, stability and certainty of the predictions following the order Spec-lab>Spec-field>Sentinel-2 BOA. This was denoted by lower R^2_{test} and RPD_{test}, higher $RMSE_{test}$ and wider CI. MeanR^2_{test}, RPD_{test} and $RMSE_{test}$ values were similar to their respective mean values of $RMSE_{cv}$ and $RMSE_{cal}$ for all variables and models built with the different reflectance datasets (Table 4). The mean systematic error given by the bias was negligible for all predictions. Therefore, the precision of the predictions (SEP_{test}) (data not shown) was very similar to their accuracy ($RMSE_{test}$).

For all reflectance datasets, the prediction ability of CP content was relatively moderate, with RPD_{test} mean values always over 1.50. Compared to the values obtained with Spec-lab reflectance (mean R^2_{test} = 0.68), the mean R^2_{test} decreased by 0.11 with Spec-field and by 0.18 when Sentinel-2 BOA reflectance was used. The difference of the R^2_{test} mean value between models fitted with Spec-field reflectance (R^2_{test} = 0.57) and models built with Sentinel-2 BOA reflectance (R^2_{test} = 0.50) was marginal. However, Fig. 4. (b) shows that the density distribution of R^2_{test} and RPD_{test} for CP predictions using Sentinel-2 BOA are specially flattened, presenting a wide CI, which indicates lower stability and certainty of the predictions. The average accuracy of the prediction, denoted by the mean $RMSE_{test}$ were 0.11, 0.13 and 0.11 (log-transformed values) for models built with Spec-lab, Spec-field and Sentinel-2 BOA reflectance respectively. Note that although the mean $RMSE_{test}$ of the models fitted with Spec-field was higher than the mean $RMSE_{test}$ of Sentinel-2 BOA models, the range of the data used has to be considered when comparing both models, being 0.86 for values used with Spec-lab and Spec-field vs 0.67 for reference data used with Sentinel-2 BOA reflectance (Table 4).

R^2_{test} and RPD_{test} statistics for NDF were worse than those obtained for CP using Spec-lab and Spec-field and very similar when Sentinel-2 BOA reflectance was used. Predictions made with Spec-lab reported a moderate predictive ability with mean R^2_{test} = 0.64 and mean RPD_{test} = 1.73. The mean values of R^2_{test} and RPD_{test} using Sentinel-2 BOA reflectance (mean R^2_{test} = 0.50 and mean RPD_{test} = 1.54) were marginally better than the values obtained for predictions made with Spec-field (mean R^2_{test} = 0.48 and mean RPD_{test} = 1.43). However, it can be observed in Fig. 4(b) that the distribution of R^2_{test} and RPD_{test} for Sentinel-2 BOA data is more flattened and has wider CIs, indicating lower stability and certainty of the predictions than those made with Spec-field.

For the rest of the variables, only predictions made with Spec-lab produced acceptable results. In the case of EDOM, the mean values obtained for R^2_{test} (0.68) and RPD_{test} (1.84) were similar to those obtained for CP predictions. Weak predictions were obtained for ADF and EDOM with Spec-field reflectance and especially with Sentinel-2 BOA data, showing very low predictive ability with mean values of R^2_{test} = 0.30 and RPD_{test} = 1.30.

3.3. Sentinel-2 bands contribution to pasture quality PLS models

The importance of the Sentinel-2 bands using Spec-lab, Spec-field and Sentinel-2 reflectance to predict CP, NDF, ADF and EDOM are

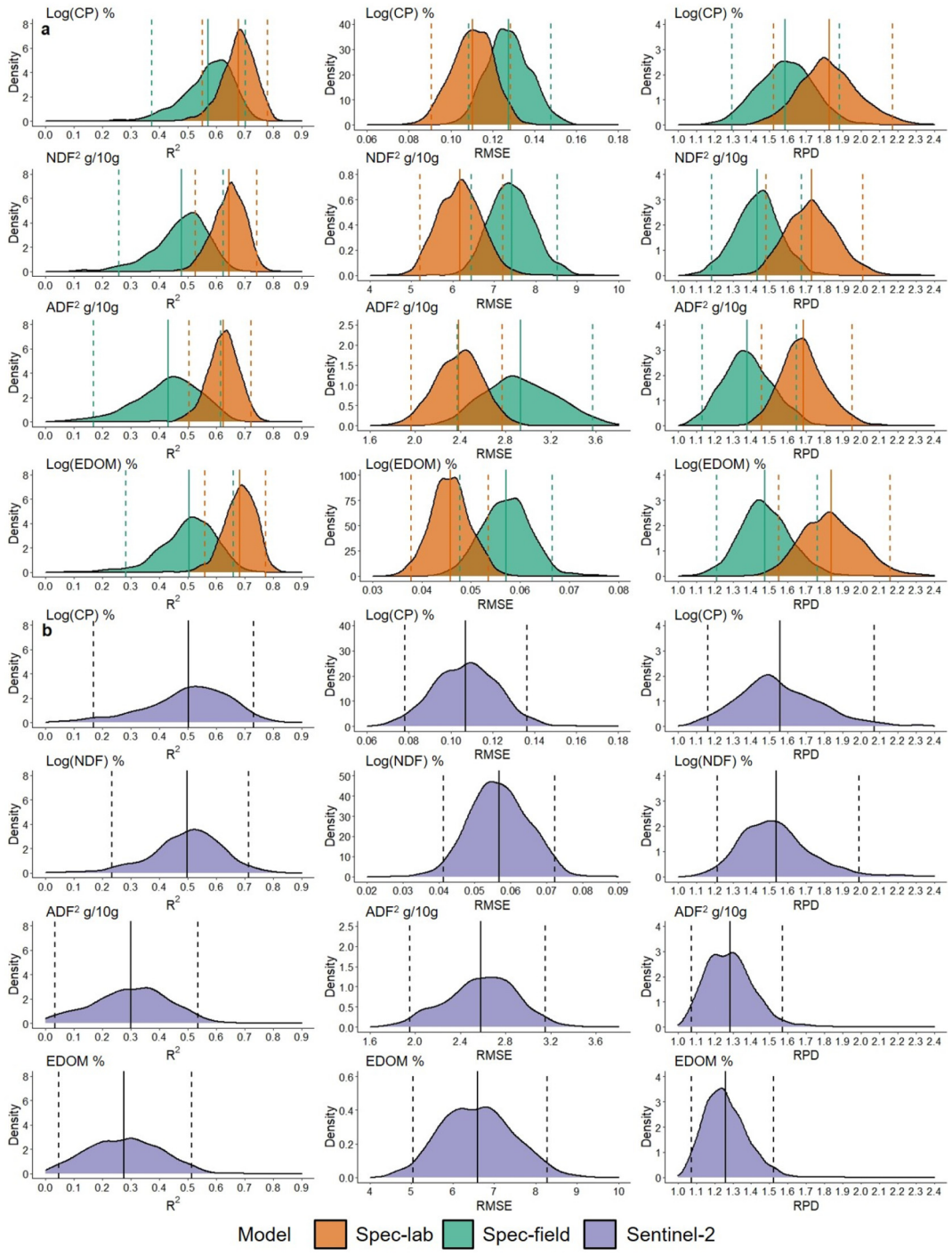

Fig. 4. Density distribution of R2, root mean square error (RMSE) and ratio of predicted deviation (RPD) of predictions over Spec-lab and Spec-field test data ($N = 49$) (a) and Sentinel-2 test data ($N = 20$) (b). Calculated from $N = 1000$ random partitions of the dataset. The predicted parameters are; crude protein (CP), neutral detergent fibre (NDF), acid detergent fibre (ADF), and enzyme digestibility of organic matter (EDOM). Solid lines show the mean and dashed lines show the confidence intervals (2.5 and 97.5 percentiles). A different transformation was applied to NDF and EDOM for Sentinel-2 dataset.

presented in Figs. 5 and 6. Main attention will be focused on those models that reported better predictive accuracy and precision. To assess CP using Spec-lab, the bands of the Red-edge region, band 7 (783 nm), band 6 (740 nm), and especially band 5 (705 nm) showed, together with band 12 (SWIR-2, 2190 nm), the greatest coefficients and therefore impact on the predictions. All these bands were significant in most of the 1000 PLS models built for this dataset with the bootstrap procedure. The bands 4 (red, 665 nm) and 8a (narrow NIR, 865 nm) also showed influence on the PLS predictions, although the coefficients were inferior and the percentage of models in which these bands resulted significant were lower: 75.7% and 73.8% respectively. For the prediction of CP with Spec-field, the red-edge region and the band 4 (red, 665 nm) also showed a great influence on the prediction. As well as with Spec-lab, the band 5 (red-edge-1, 705 nm) had the greatest coefficient for CP prediction. The main difference between models built with Spec-lab and models built with Spec-field was in the SWIR region (bands 11 and

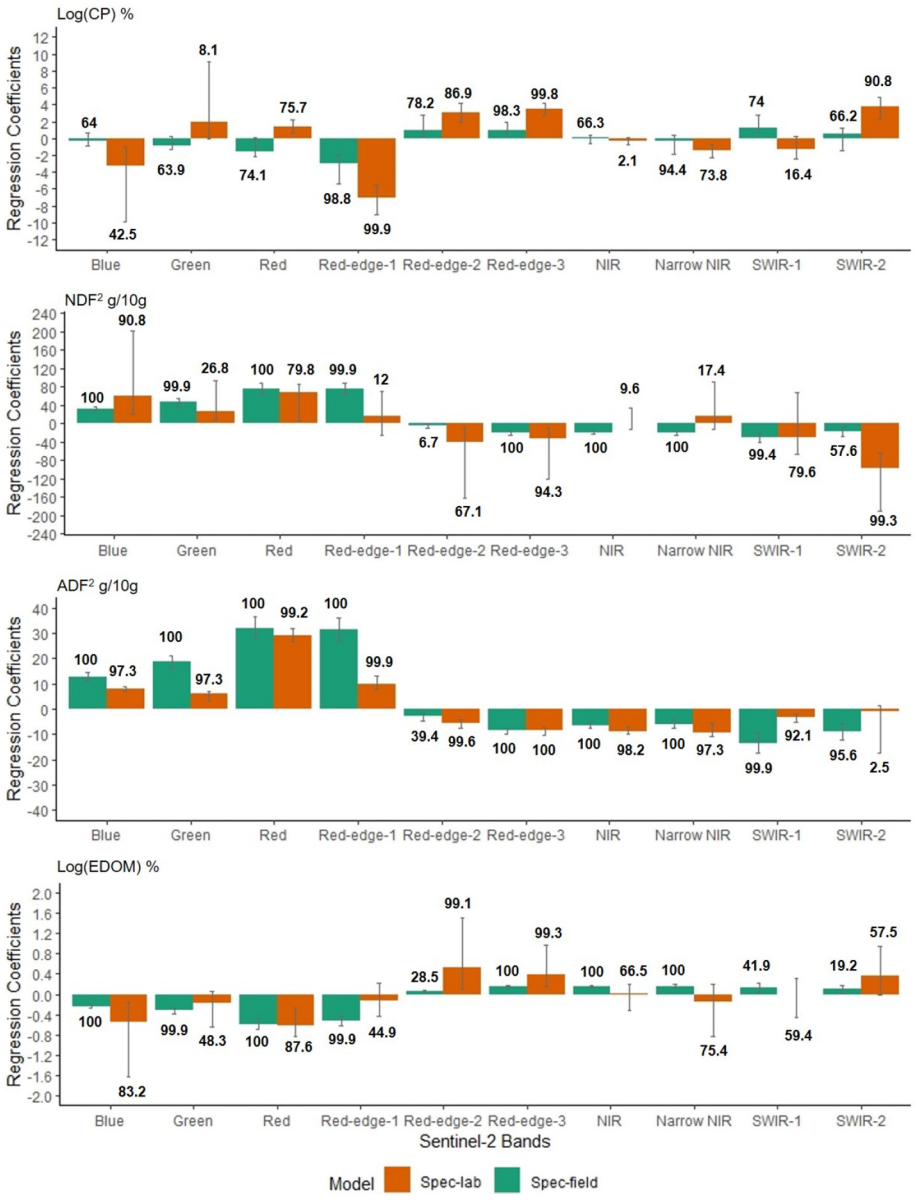

Fig. 5. Regression coefficients averaged over N = 1000 PLS models fitted with Spec-lab and Spec-field data. CP- Crude protein; NDF- neutral detergent fibre; ADF- acid detergent fibre; EDOM- enzyme digestibility of organic matter. Error bars indicate the confidence intervals (2.5 and 97.5 percentiles). Numbers indicate the percentage of PLS models in which this band resulted as significant based on jack-knifing procedure.

12). While for most of the PLS models of Spec-lab the band 11 (SWIR-1, 1610 nm) was not significant, for models built with Spec-field this band was significant in 74% of the models. The opposite occurred with the band 12 (SWIR-2, 2190 nm). In the case of the models fitted with Sentinel-2 BOA reflectance data for CP prediction, the most important bands for the predictions, as well as in models of Spec-field (Fig. 5), were bands 4 (red, 665 nm), 5 (red-edge-1, 705 nm) and 11 (SWIR-1, 1610 nm) (Fig. 6).

Bands 2 (blue, 490 nm), 4 (red, 665 nm) and 12 (SWIR-2, 2190 nm) were the most relevant for NDF prediction in models built with Spec-lab. Bands 7 (red-edge-3, 783 nm), and 11 (SWIR-1, 1610 nm) were also important. However, the CI of the bands was considerably wide. For the predictions of the fibres with Spec-field, all bands but the bands 6 (red-edge-2, 740 nm) and 12 (SWIR-2, 2190 nm) for NDF and the band 6 for ADF reported high coefficients, being significant in almost all the 1000 PLS models built. The most important bands were located at the visible region (bands 2, 3 and 4) and the band 5 (red-edge-1, 705 nm). The bands 2 and 4 from the visible region together with band 6 (red-edge-2, 740 nm) and 11 (SWIR-1, 1610 nm) had the maximum importance on the PLS models developed for NDF with Sentinel-2 BOA data.

Regarding the predictive model of EDOM, only models run with Spec-lab reported acceptable statistics, the bands 2 (blue, 490 nm) and 4 (red, 665 nm) from the visible region and 6 and 7 from the red-edge region being the most important bands in the models.

3.4. Calibration of Sentinel-2 model based on field spectrometry

The result of the PCA performed with canopy reflectance spectra recorded in situ (Spec-field) and Sentinel-2 BOA from satellite images are presented in Fig. S2. Both datasets showed overlap, which indicates that they are in the same spatial location. The three first principal components were used to calculate the DMH as they explained 99% of the

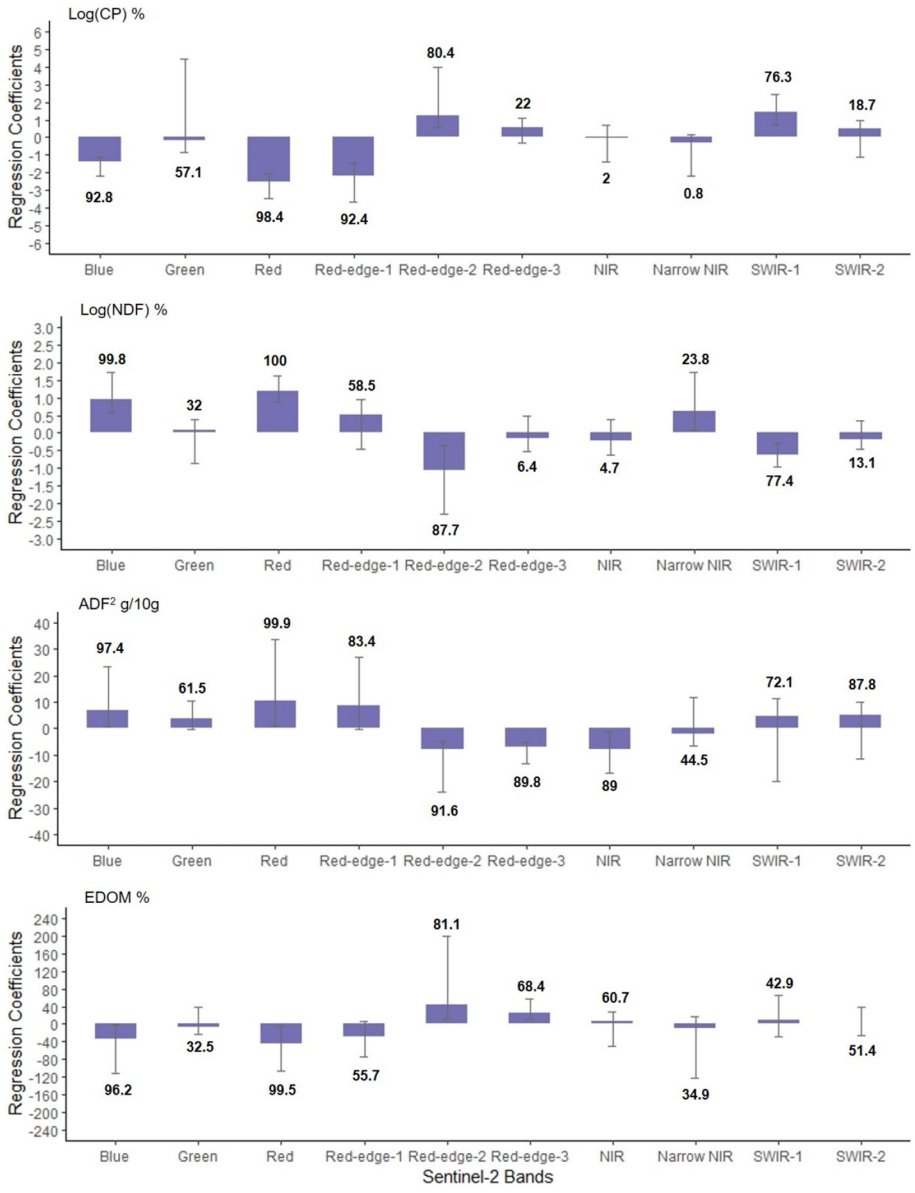

Fig. 6. Regression coefficients averaged over N = 1000 PLS models fitted with Sentinel-2 data. CP- Crude protein; NDF- neutral detergent fibre; ADF- acid detergent fibre; EDOM- enzyme digestibility of organic matter. Error bars indicate the confidence intervals (2.5 and 97.5 percentiles). Numbers indicate the percentage of PLS models in which this band resulted as significant based on jack-knifing procedure.

variance. The DMH to the centre of the population of calibration (Spec-field) was always below 3.

Calibration and cross-validation statistics of the models built with the Spec-field reflectance dataset are presented in Table 5. Moderate performance was obtained for the model calibrated for CP with R^2 = 0.60 and RPD = 1.59 of cross-validation. Weak models were produced for the rest of the variables.

Fig. 7 shows the predicted vs measured plots for each pasture quality variable (CP, NDF, ADF and EDOM) of the test set corresponding to the Sentinel-2 BOA reflectance data. As for the cross-validation, only predictions of CP reported statistics with values close to "moderate" predictive ability with RPD value over 1.50 and R^2 of 0.54. The rest of the models for NDF, ADF and EDOM showed poor predictive ability with RPD values below 1.40 and high RMSE values that indicate low prediction accuracy.

According to the thresholds to classify spatial prediction models previously explained (Askari et al., 2019), being "moderate" = 1.5 ≤ RPD < 2 and R^2 ≥ 0.60, and the results obtained for the different variables (Table 5), only maps for CP were generated. Spatial predictions of CP

Table 5
Summary statistic of calibration models fitted with Spec-field data to predict over Sentinel-2 data.

Spectral data	Variable	n	Mean	nLV	R2 cal	RMSE cal	R2 cv	RMSE cv	RPD cv
Spec-field	Log (CP) %	173	1.04 [0.87]	3	0.62	0.12	0.60	0.13	1.59
	NDF²g/10 g	173	27.45 [44.72]	3	0.49	7.45	0.46	7.64	1.37
	ADF²g/10 g	173	10.24 [17.59]	3	0.48	2.86	0.45	2.93	1.36
	Log (EDOM) %	173	1.76 [0.351]	3	0.51	0.057	0.49	0.059	1.40

CP-Crude protein; NDF-neutral detergent fibre; ADF-acid detergent fibre; EDOM-enzyme digestibility of organic matter; Mean - average of measurements with range in squared brackets; NLV- number of latent variables; RMSE- root mean square error; RPD-ratio of predicted deviation; cal- calibration statistics; cv-cross-validation statistics.

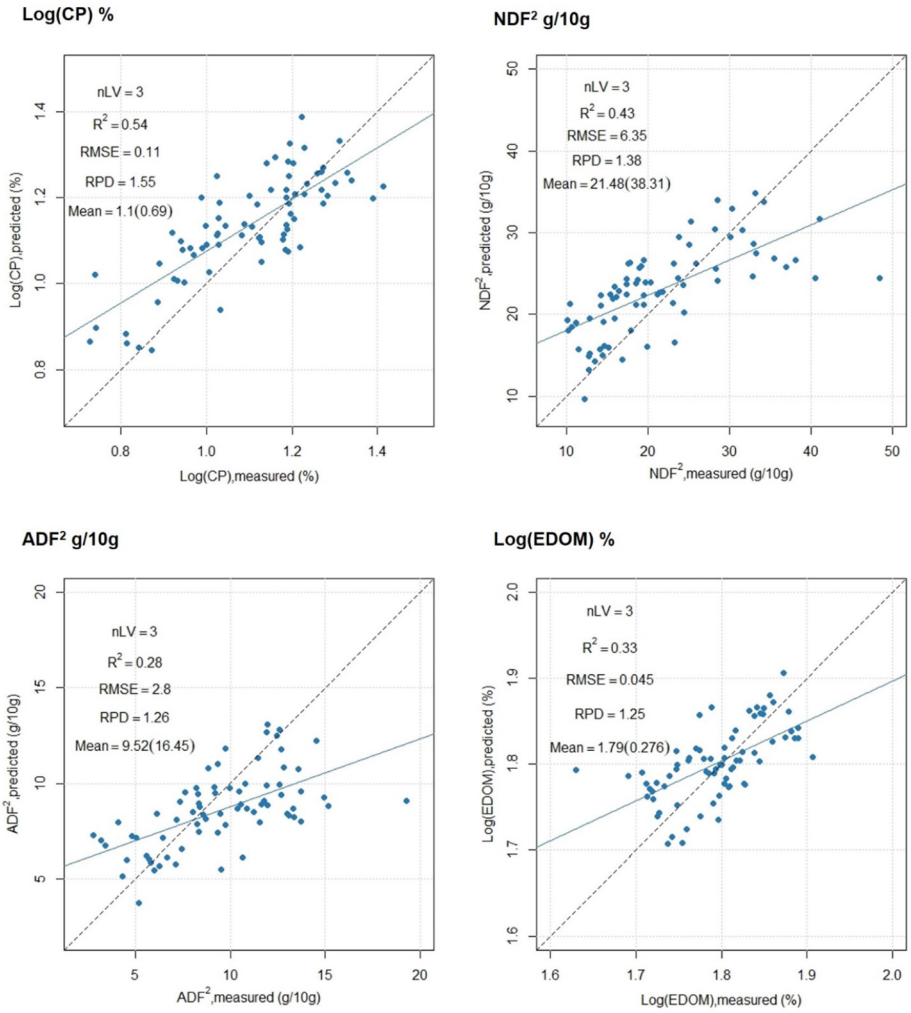

Fig. 7. Predictions of CP-Crude protein; NDF- neutral detergent fibre; ADF- acid detergent fibre; EDOM- enzyme digestibility of organic matter using PLS models fitted with Spec-field data (Table 4) and Sentinel-2 data for prediction (N = 75). Mean - average of measurements with range in brackets; nLV- number of latent variables; RMSE- root mean square error; RPD- ratio of predicted deviation. Dashed line represents the 1:1.

based on Sentinel-2 images in fields of irrigated and natural grasslands from farm 5 on different dates are presented in Fig. 8. Differences over time and between fields can be observed. In November (2018-11-13), at the beginning of the growing season, natural grasslands had higher CP content (18–14%) than irrigated grasslands (14–10%). On the next date, in April (2019-04-04) when pastures were at the peak of growth, both fields showed similar CP content (20–16%). From that date, the CP content in the field of natural grasslands drops to values below 6% in June (2019-06-28) whereas the irrigated field keeps CP values over 12%. It can also be observed that the CP content in the irrigated field is more homogeneous than in natural grasslands (Fig. 8).

4. Discussion

4.1. Potential of Sentinel-2 configuration for estimating pasture quality and modelling approach used

This study explored the potential of Sentinel-2 configuration to assess pasture quality in high-diversity grasslands of *Dehesa* systems using PLS models. The values of the pasture quality variables analysed (Table 3) fall within the usual range of pasture quality parameters of Mediterranean permanent grassland in *Dehesa* systems (Perez Corona et al., 1998; Vázquez-De-Aldana et al., 2008). We used three different reflectance datasets to investigate the capabilities of Sentinel-2 configuration to predict pasture quality. Since Vis-NIRS techniques with the whole spectral range (350–2500 nm) are used in laboratories for the chemical analysis of the variables studied here, the use of Spec-lab reflectance allowed to identify the maximum potential to establish a relationship between pasture quality variables and reflectance for Sentinel-2 bands. This reflectance data is free of factors such as water content or soil and atmospheric influences that affect field in-situ canopy reflectance and satellite-based predictions (Mansour et al., 2012). Therefore, the results obtained using Spec-lab reflectance help to inform the maximum accuracy that might be achieved with Sentinel-2 configuration for predictions of the quality variables for the studied pastures. According to Viscarra Rossel et al. (2006), models with RPD values between 1.4 and 1.8 could be used for assessment and correlations while values over 1.8 may indicate that quantitative predictions are possible. The mean RPD_{test} values obtained with Spec-lab were 1.84 for EDOM and 1.82 for CP. Lower values were obtained for the fibres, with 1.73 for NDF and 1.68 for ADF. These results illustrate that the potential of Sentinel-2 configuration to predict pasture quality in Mediterranean permanent grasslands may be limited to moderate prediction models that could allow qualitative assessments. The mean R^2_{test} values ranged between 0.68 and 0.64, which is considerably lower than R^2 values obtained for predictions of pasture quality variables using the whole spectral range (García-Ciudad et al., 1993). Although Sentinel-2 configuration has improved the spectral and temporal characteristics

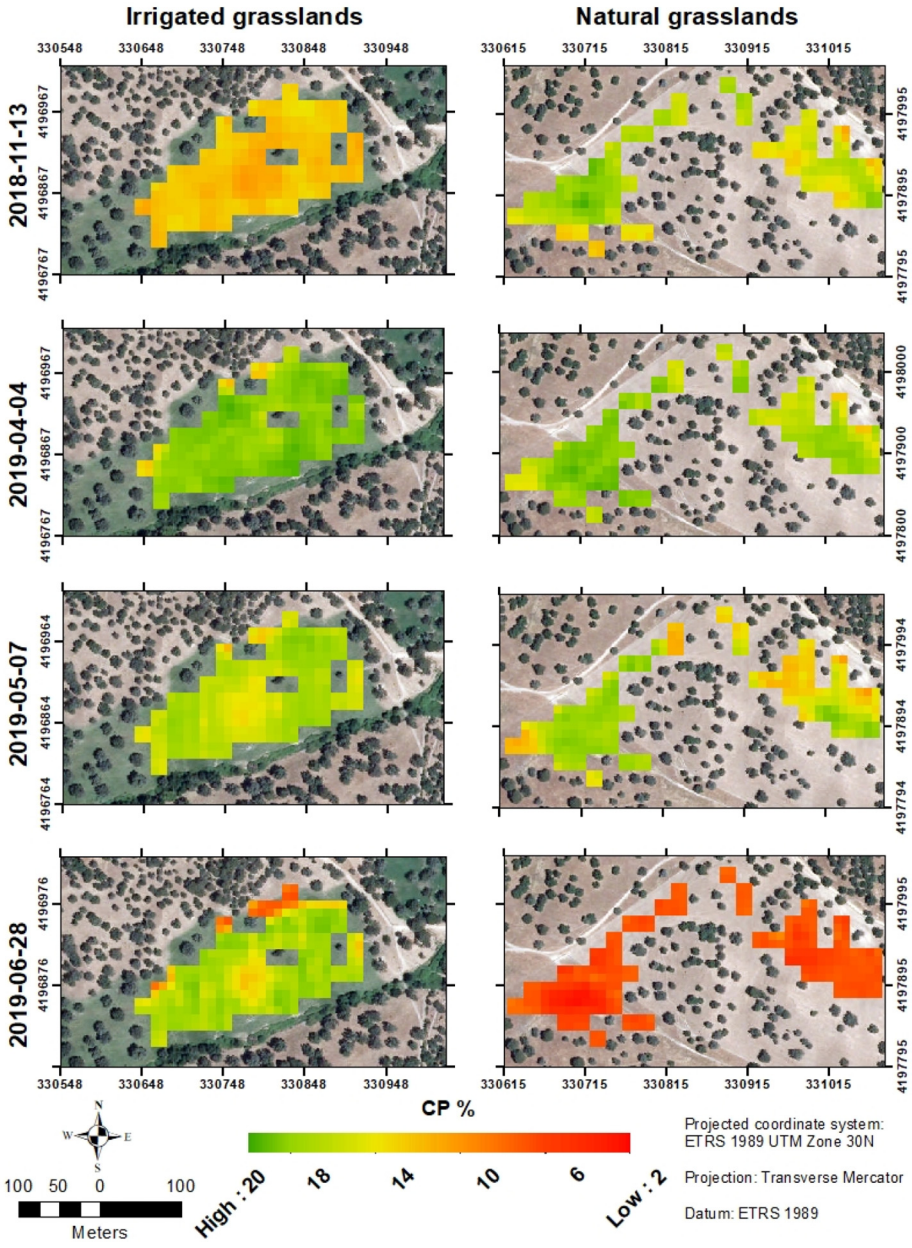

Fig. 8. Spatial predictions of crude protein (CP) for four different dates in fields of irrigated and natural grasslands in farm 5. Predictions made using a PLS model fitted with Spec-field data (Table 5) and Sentinel-2 images for prediction. Source: Background image; aerial orthophotography at 0.5 m resolution from July of 2016 (Linea, 2020).

compared with Landsat and SPOT to assess biophysical variables in vegetation (Frampton et al., 2013), the reduced spectral resolution is a basic limiting factor to obtain precise quantitative predictions. This limitation needs to be considered when planning the tool to be used for pasture quality assessment in order to adjust the specifications to the precision required. For example, Askari et al. (2019) reported better predictions of CP in mixtures of clover (*Trifolium repens* L.) and perennial ryegrass (*Lolium perenne*) using hyperspectral imagery (R^2_{cv} = 0.82 and RPD_{cv} = 2.51) compared to the predictions made with Sentinel-2 imagery (R^2_{cv} = 0.62 and RPD_{cv} = 1.60). However, as the same authors stated, the cost of acquiring hyperspectral images is a major limiting factor for the evaluation of grassland (Askari et al., 2019; Mansour et al., 2012) and it might not compensate for the increment of precision. The high-priority candidate mission of the European Space Agency: Copernicus Hyperspectral Imaging Mission for the Environment (CHIME) (Nieke and Rast, 2018) is expected to deliver a new-generation imaging spectrometer. That hyperspectral spectrometer will cover the full spectral range between 400 and 2500 nm with contiguous narrow bands at a spatial resolution similar to Sentinel-2 (30–60 m) (Nieke and Rast, 2018). This new generation of hyperspectral satellites could overcome the constrain of the spectral coverage of multispectral satellites and allow the improvement of grasslands quality assessments from qualitative to quantitative (Rast et al., 2019). Another constraint for the remote sensing of permanent grasslands in open woodland as *Dehesa* and *Montado* is the presence of scattered trees. The spatial resolution of Sentinel-2 forces to seek open pasture areas where there is no influence of trees on the pixel reflectance. This tool could have no possibility of application in *Dehesa* and *Montado* farms with high tree cover and no open areas. A feasible option might be the analysis of pixels as representative observations in sampling areas without tree cover that could characterise the status of the rest of the grassland. However, the information provided might not be representative of the pasture below the canopy since

its phenology and quality might differ from the pasture beyond the tree canopy (López-Carrasco et al., 2015). Other satellite constellations with finer spatial resolution such as WorldView-2 (Adjorlolo et al., 2015) or the use of aircraft vehicles (Askari et al., 2019; Lu and He, 2017) could partially overcome this limitation and provide more data although at a higher cost. The development of pasture quality maps using Sentinel-2 imagery is restricted to areas without trees (see 4.3. Use of field spectrometry for Sentinel-2 model calibration and pasture quality mapping). Further research is needed to isolate the influence of tree canopy reflectance in pixels partially covered by trees.

One of the factors affecting the prediction accuracy and model performance is the high species diversity of the permanent grasslands analysed in this study. Heterogeneous pastures with multiple functional groups and different phenological stages might produce confounding effects on the relationship between pasture quality variables and reflectance (Fava et al., 2009; Kattenborn et al., 2019; Tong and He, 2017; Zhou et al., 2019). This factor is expected to be especially important when using canopy reflectance and satellite imagery. Differing leaf area index of grassland communities with multiple species may affect the canopy reflectance and therefore the potential to estimate plant components (Kattenborn et al., 2019; Pellissier et al., 2015). In fact, one of the main limitations for remote-sensing of foliar chemistry is that the chemical composition can be confounded by phenology or canopy geometry (Curran, 1989). Contrasting results have been obtained when developing predictive models for specific pastures and/or development status. Biewer et al. (2009) reported improved estimates of CP by using legume-specific calibrations. Zhou et al. (2019) did not find any influence of mixture types and developmental stages on CP predictions, although the pastures studied were less heterogeneous. Zeng and Chen (2018) obtained greatly improved estimates of CP, NDF, and ADF in wheatgrass communities when data from different growth stages were included in the models compared to those developed with data from individual growth stages. However, the differences may be attributed to the wider range of the dataset. Our study provides an overview of the potential of generalised models to predict forage quality in Mediterranean permanent grasslands using samples from high-diversity and different phenological stages. Further research is needed to explore the possibilities to improve predictions using separate prediction models for specific phenological stages or mixtures in high-diversity Mediterranean grasslands. The differences in model performance of Spec-lab-based models and models built with Spec-field and Sentinel-2 BOA seem also to point to the influence of water content, leaf area index and soil background. Although these factors were not explicitly investigated in this study, canopy reflectance spectra is clearly affected by the presence of bare soil over the target areas (Atzberger and Richter, 2012; Jacquemoud et al., 2009; Mansour et al., 2012; Yue et al., 2020). Soil moisture and plant water content can also be a source of noise in the reflectance spectra of Spec-field and Sentinel-2 (Kokaly, 2001; Ramoelo et al., 2011). Water absorbs in similar regions of the spectra than other organic compounds, which results in a combined or masked effect on the reflectance (Kokaly, 2001). For example, the O—H is a common absorption bond for water and lignin (Curran, 1989). The controlled condition in which Spec-lab reflectance data was acquired and the use of ground dried samples prevents it from introducing this noise. Overall, the differences in mean R^2_{test} and mean RPD_{test} values between models built with Spec-field and models constructed with Sentinel-2 were marginal. This might indicate a low influence of the atmospheric interference in Sentinel-2 BOA data. However, the CIs of the predictions made with Sentinel-2 denote a higher uncertainty of these models. The differences between models run with Sentinel-2 data and Spec-field can be also affected by the different number of samples. The higher number of samples of Spec-field dataset (173) compared to Sentinel-2 BOA dataset (75) may account for the narrower CIs in models built with Spec-field, which allowed the development of more robust models. Another factor influencing the accuracy and prediction ability of models constructed with Sentinel-BOA data might be the sample collection. Since the reference measurements used are a mean value of four samples, a standard error is associated to this value. Thus, the selection of homogeneous areas with common management and a suitable sampling design are essential to reduce the degree of uncertainty (Raab et al., 2020).

Calibrations built to predict NDF and especially CP showed promising test results that suggest the possibility of performing qualitative assessments based on Sentinel-2 imagery. The mean R^2_{test} obtained for CP predictions using Spec-field reflectance was similar to previously reported values. Ramoelo et al. (2015) obtained values of $R^2 = 0.46$ in cross-validations of PLS models of 5 LV to predict leaf nitrogen in rangelands using field in-situ reflectance resampled to Sentinel-2 configuration. Adjorlolo et al. (2015) obtained $R^2 = 0.50$ in cross-validation of PLS models fitted with field canopy reflectance resampled to WorldView-2 band settings to predict CP in grassland communities of *Festuca costata*, *Themeda triandra* and *Rendlia altera*. Also, similar values of R^2 (0.60) in cross-validations were reported by Kawamura et al. (2008) in PLS models with 7 LVs using the whole spectral range (400–2350 nm) and band selection procedures to predict CP in mixed sown pastures. Askari et al. (2019) obtained slightly better cross-validation statistics ($R^2 = 0.62$ and $RPD = 1.60$) using Sentinel-2 imagery and PLS models to predict CP compared to the test results of our study (mean $R^2_{test} = 0.50$ and mean $RPD_{test} = 1.56$), although the homogeneity of the studied pasture (a mixture of clover and perennial ryegrass) may explain the improved results.

Few studies have investigated the potential of Sentinel-2 configuration to assess fibre content in pastures. We obtained mean $R^2_{test} = 0.48$ and mean $RPD_{test} = 1.43$ using Spec-field to predict NDF. Lower statistics (bootstrapped mean $R^2 = 0.31$) in PLS models to predict NDF were obtained by Kawamura et al. (2008) using the whole spectral range (400–2350 nm, resampled at 5 nm) and band selection, whereas Zeng and Chen (2018) reported improved R^2 values of 0.77 and 0.80 for NDF and ADF using data of three different growth stages. Acceptable values were reported by Adjorlolo et al. (2015) ($R^2 = 0.52$) with field spectroscopy and WorldView-2 configuration to predict NDF. We obtained similar goodness to fit using Sentinel-2 BOA imagery (mean $R^2_{test} = 0.50$). The poor results obtained for ADF predictions contrast with the results of the studies mentioned above. Raab et al. (2020) reported high R^2 values (0.79) from ADF predictions using Sentinel-2 and Sentinel-1 data and random forests regressions algorithms. The inclusion of radar data from Sentinel-1 could contribute to estimating ADF since it provides information of the height of the pasture, which is directly related to the cellulose and lignin content. The same study also obtained good predictive models for CP ($R^2 = 0.72$). The authors state that Sentinel-2 data might be sufficient to predict forage quality (Raab et al., 2020), thus the improved results could respond to the use of the random forest algorithm along with the higher homogeneity of the grasslands studied and the dense temporal component of their dataset. They also demonstrated that the inclusion of indices and simples ratios combined with variable selection techniques can significantly improve the prediction accuracy of the models (Raab et al., 2020). Although the addition of several indices and ratios together with single bands can lead to multicollineality problems, variable selection techniques can overcome this problem while improving the prediction ability of the models (Belgiu and Drăguţ, 2016; Frenich et al., 1995; Kawamura et al., 2008; Raab et al., 2020; Santos-Rufo et al., 2020). Ramoelo et al. (2015) also obtained better results predicting nitrogen content by using random forest ($R^2 = 0.90$ and $RMSE = 0.04$) than with PLS regression ($R^2 = 0.46$ and $RMSE = 0.14$). We decided to use PLS regression for the sake of simplicity and to ease the interpretation of results. The PLS models were easy to calibrate and the results were also simple to understand. The similar results between cross-validation and test indicated that there was no overfitting of the models. Machine-learning techniques such as random forest or support vector machine could be an asset to detect the non-linear relationship between pasture quality and canopy reflectance (Zhou et al., 2019). However, these techniques

can be sensitive to complex modelling approaches (Igne et al., 2010) while techniques such as PLS regression are simpler to implement and compute (Askari et al., 2019), which might facilitate its use by consultancies and grasslands managers. Studies comparing PLS, random forest and support vector machine could be helpful to find the optimal model to implement with Sentinel-2 data in terms of accuracy and ease of use. Finally, although EDOM of pasture is positively correlated to CP and negatively to NDF and these two variables were acceptably predicted, weak results were obtained for EDOM. The reasoning behind this could be that EDOM is not a variable directly related to a nutrient of the plants as is the case of CP with nitrogen, but rather it is a result of the fibre and CP content. This, together with the differences in digestibility of the multiple species/ functional groups and their phenology in the sampled grasslands could account for the bad predictions of this variable using Spec-field and Sentinel-2 BOA.

The wide range of the data acquired from 8 different farms allowed us to capture the variability of *Dehesas* grasslands and provide a representative modelling of this ecosystem. We highly recommend the implementation of a bootstrap approach to assess the stability and certainty of the predictive models (Mutanga et al., 2004; Mutanga et al., 2015). Relatively small sample sizes are used in this kind of study, typically around 100 samples (Askari et al., 2019; Kawamura et al., 2008; Mutanga et al., 2004; Raab et al., 2020). As can be observed in Fig. 4, the wide confidence intervals denote high variability in the results depending on the corresponding partition, especially for Sentinel-2 BOA reflectance data, whose sample size was 75 compared to the 173-sample size of Spec-lab and Spec field. Reporting a single value of RMSE, R^2 and RPD could lead to biased conclusions since it does not provide information about the certainty of the results (Mutanga et al., 2004). We obtained values of R^2_{test} ranging from 0.1 to 0.8 for CP using Sentinel-2 BOA reflectance. Kawamura et al. (2008) and Mutanga et al. (2004) reported similar bootstrapped values of R^2 from CP and nitrogen content predictions with canopy spectral measurements. We extended this approach to the analysis of the regression coefficients which allowed us to delimitate the certainty of the values of these coefficients as well as the stability of the bands, and therefore permitted a more reliable interpretation of the bands' importance.

Using large and representative datasets that include a wide range of variation of the studied variable is key to reducing the uncertainty and improving the accuracy of the predictive models (Norris and Barnes, 1976). However, the data collection and reference measurement determination can be challenging. Given the growing interest in predictive models of forage quality in grasslands using remote sensing applications, the development of public reflectance spectral libraries from different studies could make available large datasets to improve calibrations. The use of national libraries has been successfully applied for soil property characterization using Vis-NIRS spectroscopy (Knadel et al., 2012; Liu et al., 2018; Shepherd and Walsh, 2002).

4.2. Sentinel-2 bands importance on pasture quality assessment

The mean regression coefficients (average of 1000 values) were used to assess the bands' importance on the predictions of pasture quality variables (CP, NDF, ADF and EDOM) using PLS regression. For the prediction of CP, band 4, the red-edge and the SWIR regions had the greatest impact on the predictions. This was common for all of the three reflectance datasets. Band 5 (705 nm) proved to be especially important for CP prediction. These results are in accordance with previous studies that highlighted the importance of the red-edge region (700–775 nm) and wavelength reflectance between 1200 and 2400 to estimate CP using ground-based canopy reflectance (Adjorlolo et al., 2015; Kawamura et al., 2008; Kokaly, 2001; Ramoelo and Cho, 2018). Ramoelo et al. (2015), using Sentinel-2 simulated data to predict nitrogen content in rangelands, also noted the importance of bands 4 (665 nm), 5 (705 nm) in the red and red-edge region and bands 11 (1610 nm) and 12 (2190 nm) in the SWIR region. Raab et al. (2020) reported simple ratios based on the red-edge region as particularly important to predict CP. The importance of the red-edge region relies on the correlation between CP (closely related to nitrogen content) and chlorophyll concentration (Curran, 1989; Pellissier et al., 2015; Raab et al., 2020; Tong and He, 2017), whereas the importance of the SWIR region respond to absorption due to C—H, N—H, O—H and C—O bonds (Adjorlolo et al., 2015; Curran, 1989; Curran et al., 1992; Kawamura et al., 2008; Kokaly, 2001). Other studies using Sentinel-2 data have also informed of bands from the visible region (band 3 and band 4) and narrow-NIR (band 8a) as useful bands for CP prediction (Askari et al., 2019; Lugassi et al., 2019).

The differences in the importance of band 12 (SWIR-2, 2190 nm) between models built with Spec-lab and models constructed with Spec-field and Sentinel-2 BOA reflectance could be attributed to the plant water content and soil background effect (Mansour et al., 2012). SWIR absorption is affected by the reflectance of leaf water content, masking reflectance features of other biochemicals, which influence the accuracy of the predictions (Ramoelo et al., 2011). Ripple (1986) pointed out that the spectra reflectance region 2080–2350 nm shows sensitivity to changes in both soil background and relative water content of leaves. Since the Spec-lab data had no noise from water content or soil, the reflectance at band 12 had a great impact on the prediction of CP and NDF. The reflectance of Spec-field and Sentinel-2 could be affected by these two factors resulting in a confounding effect to predict CP or NDF that produced a low regression coefficient. Adjorlolo et al. (2015) informed that the most highly-ranked waveband for predicting CP using in situ canopy reflectance and PLS regression was centred at 2280 nm. Differences between studies might lie in the effect of soil background reflectance. The extent of the influence of soil reflectance on pasture quality prediction might be worth investigating in further research since it seems to be one of the main factors affecting the performance of the predictions.

Concerning the importance of bands for NDF prediction using Spec-lab data, the selection of bands of the visible region (bands 2, blue and 4, red) together with the SWIR region and to a lesser extent the red-edge band 7 is in accordance with previous studies (Kawamura et al., 2008). The models built with Sentinel-2 BOA reflectance also presented high regression coefficients in bands 2 and 4 and the red-edge band 6 coinciding with results obtained for Spec-lab. However, band 12 as well as for CP had lower coefficients, possibly due to the effect of water of soil background as discussed above. Bands 2 and 4 impact on fibre prediction might be related to the detection of pigments in different phenological stages of the pasture (Mansour et al., 2012; Ustin et al., 2009). Bands of the SWIR region have been widely selected for fibre determination (García-Ciudad et al., 1993), due to the overtones C—H, C—N and N—H, closely related to fibre components (Clark and Lamb, 1991). The regression coefficients of models fitted with Spec-field also showed great impact on the visible region and band 5 (705 nm) although the weaker calibrations could have affected the regression coefficients as happened for ADF and EDOM using Spec-field and Sentinel-2 BOA reflectance.

4.3. Use of field spectrometry for Sentinel-2 model calibration and pasture quality mapping

As discussed previously, the creation of suitable datasets of pasture quality samples and reflectance libraries will be key to developing effective and efficient Sentinel-2 based predictive models. However, the collection and analysis of samples is tedious and expensive (Starks et al., 2006). Here, we explored the option of using field canopy reflectance resampled to the Sentinel-2 configuration to calibrate models that could be used in combination with Sentinel-2 imagery. This would allow the use of samples and reflectance measurements already collected to develop robust calibrations that could then be applied to Sentinel-2 BOA images.

The PCA analysis (Fig. S2) illustrated that both datasets, Spec-field and Sentinel-2 BOA were in the same spatial location and showed representativity. All the Sentinel-2 samples showed a DMH lower than 3 to the centre of the population of calibration (Spec-field) (Fig. S2). Since in Vis-NIRS spectroscopy, DMH = 3 is generally the maximum DMH acceptable to predict new samples using a calibrated model (Shenk and Westerhaus, 1996; Williams and Sobering, 1996), these results confirm that these two datasets can be combined to perform PLS calibrations and predictions. Previous studies have used field canopy reflectance and combined it with Sentinel-2 images (Lugassi et al., 2019; Ramoelo and Cho, 2018). However, to our knowledge, the representativity of these two different datasets of reflectance has never been checked.

Only the prediction made for CP produced acceptable results that allow its use for qualitative assessments of CP (Fig. 7). To illustrate the potential application of these models, the calibrated model for CP was used to perform spatial predictions of CP (Fig. 8) showing clear differences between fields associated with their management. The reason for irrigated grasslands having lower CP content than natural grasslands (Fig. 8) is the presence of grazing cattle during the summer season in the irrigated field. By the first date of mapping, in November, at the beginning of growing, the irrigated pastures were mostly consumed with mainly stems remaining (with lower CP content than leaves). Thus, the quality is clearly lower than in natural grasslands which are starting to grow and have been reserved from grazing and therefore have higher CP content at this date. The CP maps allow identifying differences between both inter fields and intra fields. Overall, the CP content of natural grasslands is more heterogeneous. Lugassi et al. (2019), using laboratory and field spectral measurements at Sentinel-2 configuration, also found spatial heterogeneity in Mediterranean grasslands responding mainly to changes in topography.

4.4. Implications for management of open woodlands and future studies

The present study has demonstrated that qualitative assessments of CP and NDF using free-available Sentinel-2 imagery can be successfully implemented for high-diversity Mediterranean permanent grasslands. The availability of real-time data of CP and NDF content provided by Sentinel-2 imagery can be used to assess the carrying capacity of pastures, adjust stocking rates and plan the spatio-temporal livestock grazing on *Dehesa* farms (Ramoelo and Cho, 2018; Starks et al., 2006). The managers can also decide in real-time, based on the estimation of CP of the pastures, if supplementary feeding is necessary (Raab et al., 2020). It is also an inexpensive way to evaluate interventions such as grassland improvements with legume mixes or fertilisation without the need for laborious fieldwork and expensive laboratory analyses which would need to be done repeatedly. CP maps produced with Sentinel-2 imagery could help to identify patches where overseeding with legumes might be needed to improve the CP offer of *Dehesa* permanent grasslands, improving in this way the efficiency of this intervention. The possibility of performing spatial and real-time temporal monitoring is especially important on large farms where the status of pastures cannot be inspected visually by managers regularly (CSIRO, 2020).

From the point of view of policies, the Common Agricultural Policy is giving increasing importance to the provision of ecosystem services and sustainable management of European grasslands via agri-environment schemes (Harlio et al., 2019; Simoncini et al., 2019). The high revisiting time (5 days) of Sentinel-2 allows the establishment of monitoring systems based on qualitative assessments of pasture quality to provide spatial data very timely. This is especially relevant in Mediterranean permanent grasslands because of the high intra- annual changes that characterise these communities. Therefore, Sentinel-2 reveals as a promising tool to evaluate the effectiveness of the agri-environment schemes since it contributes to monitoring the conservation status, the sustainability of farming management as well as the provision of ecosystem services in Mediterranean grassland communities.

Based on the insights provided here, future studies are needed to go into detail about the remote sensing of Mediterranean permanent grasslands using Sentinel-2. In this study, we used different sources and samplings to explore the feasibility of this technique. As Raab et al. (2020) suggested, the formula by Justice and Townshend (1981) could be used to calculate the required plot size for the grassland samplings: $S = P(1 + 2L)$, where S is the length of the plot, P is the spatial resolution of the pixel and L the geolocation error. However, the plot size provided by this formula can be difficult to use in open woodlands landscapes without including a tree signal. A feasible setup could consist of calibrating robust models based on field spectroscopy and then used them to make spatial predictions with Sentinel-2 imagery. This approach can improve the match between the reflectance data and the pasture quality variables in heterogeneous grasslands while overcoming the spatial constrain of scattered trees. It also would help to reduce the uncertainty of the models by targeting the acquisition of field spectroscopy at capturing the variability of the grasslands, which might be difficult with samplings at the pixel level. Increasing the temporal domain of the dataset will be key to improve the predictions and reducing their uncertainty.

Another research gap for future studies is the comparison of different models such as PLS, random forest, support vector machine and artificial neural network and their optimisation through feature elimination methods. This could also allow the inclusion of multiple ratios and indices that might enhance the relationship between the Sentinel-2 derived data and the predicted variable. Alternative methods to PLS such as convolutional neural networks could capture strong nonlinear spectral-chemical relationships (Pullanagari et al., 2021). However, the prediction of pasture quality using Sentinel-2 data in heterogeneous permanent grasslands could be limited to a certain level regardless of the methodology implemented, and possibly the improvement compared to the results delivered by Spec-lab models would be marginal. Therefore, new sensors with finer spatial and spectral resolution could be necessary to overcome this limitation in Mediterranean permanent grasslands. Future research should aim at simulating hyperspectral data, for example, based on the specifications of the high-priority candidate mission of the European Space Agency; CHIME (Nieke and Rast, 2018), with different machine learning techniques to elucidate the level of accuracy that could be achieved.

5. Conclusion

The results obtained for models built with Spec-lab reflectance show that the potential of Sentinel-2 configuration to predict pasture quality in Mediterranean permanent grasslands using PLS models may be limited to moderate prediction ability for assessment of CP, NDF, ADF and EDOM ($1.5 \le RPD < 2$ and $0.6 \le R^2 < 0.5$) that could allow performing qualitative assessments. Models built with Sentinel-2 imagery show test results from predictions of NDF and especially CP suggesting the possibility of qualitative assessments of these parameters in Mediterranean permanent grasslands of open woodlands.

The differences in accuracy obtained for Spec-lab and those reported for both, Spec-field and Sentinel-2 BOA images point at the effects of soil background, water content of vegetation and effects of heterogeneous canopies of diverse grasslands on reflectance. Additionally, intrinsic factors associated with the structure of open woodlands such as the presence of scattered trees restrict the use of Sentinel-2 images to the management of Mediterranean permanent grasslands. Further research is needed to tackle these limitations.

In accordance with previous studies, the red-edge (especially band 5) and the SWIR regions show the highest potential for estimating CP and NDF. Bands 2, blue and 4, red also seem to be important for the prediction of NDF.

The development of large and representative datasets with a wide range of variation of pasture quality is pivotal to reducing the uncertainty and improving the accuracy of the predictive models. Using field spectroscopy in combination with Sentinel-2 imagery can contribute to developing larger datasets and more robust models.

The qualitative assessment of CP and NDF content in permanent grasslands of open woodland farms using Sentinel-2-based models is a powerful tool to improve the efficiency and sustainability of management through more informed and effective decision-making.

CRediT authorship contribution statement

Pilar Fernández-Rebollo and María P. Gónzalez-Dugo designed the experiment. Jesús Fernández-Habas, Alma María García Moreno, José Ramón Leal Murillo and Pedro J. Gómez-Giraldez carried out field work. Maria Teresa Hidalgo-Fernández and José Ramón Leal Murillo carried out the sample handling and spectral laboratory measurements. Alma María García Moreno and Pilar Fernández-Rebollo helped with technical aspects of field data collection and spectral laboratory measurements. Jesús Fernández-Habas performed data analysis, built the PLRS models and drafted the manuscript. Begoña Abellanas Oar and Pilar Fernández-Rebollo assisted with building of PLSR models. All authors contributed to reviewing all drafts of the manuscript.

Declaration of competing interest

The authors declare that they have no known competing financial interests or personal relationships that could have appeared to influence the work reported in this paper.

Acknowledgements

This study was funded by the following projects:

Operational Group GOP2I-HU-16-0018 (Organic beef cattle production based on Pasture in *Dehesa* ecosystem: Production and Commercialisation improvement). Co-funded by the European Union and Junta de Andalucía with the European Agricultural Fund for Rural Development (EAFRD) through the Consejería de Agricultura, Ganadería, Pesca y Desarrollo Sostenible.

European Union's Horizon 2020 research and innovation programme, grant agreement 774124, project SUPER-*G* (Sustainable Permanent Grassland Systems and Policies).

SensDehesa project (PP.PEI.IDF201601.16), co-funded at 80% by the European Regional Development Fund (ERDF) as part of the Andalusian operational program 2014–2020.

The study was developed thanks to a PhD fellowship FPU (code FPU18/02876) of the Spanish Ministry of Education awarded to J. Fernández-Habas.

The authors would like to thank the anonymous reviewers for providing insightful suggestions that have allowed to significantly improve the manuscript.

Appendix A. Supplementary data

Supplementary data to this article can be found online at https://doi.org/10.1016/j.scitotenv.2021.148101.

References

Adjorlolo, C., Mutanga, O., Cho, M.A., 2015. Predicting C3 and C4 grass nutrient variability using in situ canopy reflectance and partial least squares regression. Int. J. Remote Sens. 36, 1743–1761. https://doi.org/10.1080/01431161.2015.1024893.

Ali, I., Cawkwell, F., Dwyer, E., Barrett, B., Green, S., 2016. Satellite remote sensing of grasslands: From observation to management. J. Plant Ecol. 9, 649–671. https://doi.org/10.1093/jpe/rtw005.

Askari, M.S., O'Rourke, S.M., Holden, N.M., 2015. Evaluation of soil quality for agricultural production using visible-near-infrared spectroscopy. Geoderma 243–244, 80–91. https://doi.org/10.1016/j.geoderma.2014.12.012.

Askari, M.S., McCarthy, T., Magee, A., Murphy, D.J., 2019. Evaluation of grass quality under different soil management scenarios using remote sensing techniques. Remote Sens. 11, 1–23. https://doi.org/10.3390/rs11151835.

Atzberger, C., Richter, K., 2012. Spatially constrained inversion of radiative transfer models for improved LAI mapping from future Sentinel-2 imagery. Remote Sens. Environ. 120, 208–218. https://doi.org/10.1016/j.rse.2011.10.035.

Belgiu, M., Drăguț, L., 2016. Random forest in remote sensing: A review of applications and future directions. ISPRS J. Photogramm. Remote Sens. 114, 24–31. https://doi.org/10.1016/j.isprsjprs.2016.01.011.

Biewer, S., Fricke, T., Wachendorf, M., 2009. Development of canopy reflectance models to predict forage quality of legume-grass mixtures. Crop Sci. 49, 1917–1926. https://doi.org/10.2135/cropsci2008.11.0653.

Bugalho, M.N., Caldeira, M.C., Pereira, J.S., Aronson, J., Pausas, J.G., 2011. Mediterranean cork oak savannas require human use to sustain biodiversity and ecosystem services. Front. Ecol. Environ. 9, 278–286. https://doi.org/10.1890/100084.

Camilli, F., Pisanelli, A., Seddaiu, G., Franca, A., Bondesan, V., Rosati, A., Moreno, G., Pantera, A., Hermansen, J.E., Burgess, P.J., 2018. How local stakeholders perceive agroforestry systems: an Italian perspective. Agrofor. Syst. 92, 849–862. https://doi.org/10.1007/s10457-017-0127-0.

Clark, D.H., Lamb, R.C., 1991. Near infrared reflectance spectroscopy: a survey of wavelength selection to determine dry matter digestibility. J. Dairy Sci. 74, 2200–2205. https://doi.org/10.3168/jds.S0022-0302(91)78393-8.

Cosentino, S.L., Porqueddu, C., Copani, V., Patanè, C., Testa, G., Scordia, D., Melis, R., 2014. European grasslands overview: mediterranean region. Grassl. Sci. Eur. 19, 41–56.

CSIC-IARA, 1989. Ma pa de suelos de Andalucía, (1:400.000). In: Mudarra, J.L., Barahona, E., Baños, C., Iriarte, A., Santos, F. (Eds.), Consejería de Agricultura y Pesca, Junta de Andalucía, Sevilla, Spain.

CSIRO, 2020. Pastures from Space. https://www.csiro.au/en/Research/AF/Areas/Digital-agriculture/Cropping-pastures/Pastures-from-Space.

Curran, P.J., 1989. Remote sensing of foliar chemistry. Remote Sens. Environ. 30, 271–278. https://doi.org/10.1016/0034-4257(89)90069-2.

Curran, P.J., Dungan, J.L., Macler, B.A., Plummer, S.E., Peterson, D.L., 1992. Reflectance spectroscopy of fresh whole leaves for the estimation of chemical concentration. Remote Sens. Environ. 39, 153–166. https://doi.org/10.1016/0034-4257(92)90133-5.

Defourny, P., Bontemps, S., Bellemans, N., Cara, C., Dedieu, G., Guzzonato, E., ... Koetz, B., 2019. Near real-time agriculture monitoring at national scale at parcel resolution: performance assessment of the Sen2-Agri automated system in various cropping systems around the world. Remote Sens. Environ. 221, 551–568. https://doi.org/10.1016/j.rse.2018.11.007.

Dumont, B., Andueza, D., Niderkorn, V., Lüscher, A., Porqueddu, C., Picon-Cochard, C., 2015. A meta-analysis of climate change effects on forage quality in grasslands: specificities of mountain and Mediterranean areas. Grass Forage Sci. 70, 239–254. https://doi.org/10.1111/gfs.12169.

ESA, E. S. A, 2020. Level 2A Processing Overview. https://earth.esa.int/web/sentinel/technical-guides/sentinel-2-msi/level-2a-processing. (Accessed 15 June 2020).

Fauvel, M., Lopes, M., Dubo, T., Rivers-Moore, J., Frison, P.L., Gross, N., Ouin, A., 2020. Prediction of plant diversity in grasslands using Sentinel-1 and -2 satellite image time series. Remote Sens. Environ. 237, 111536. https://doi.org/10.1016/j.rse.2019.111536.

Fava, F., Colombo, R., Bocchi, S., Meroni, M., Sitzia, M., Fois, N., Zucca, C., 2009. Identification of hyperspectral vegetation indices for Mediterranean pasture characterization. Int. J. Appl. Earth Obs. Geoinf. 11, 233–243. https://doi.org/10.1016/j.jag.2009.02.003.

Fernández, P., Carbonero, M.D., García, A., Leal, J.R., Hidalgo, M.T., Vicario, V., ... González, M.P., 2014. Variación de la proteína bruta y de la digestibilidad de los pastos de dehesa debida a una supresión temporal del pastoreo. 53ª Reunión Científica de la SEEP. Potes, Spain.

Ferraz-de-Oliveira, M.I., Azeda, C., Pinto-Correia, T., 2016. Management of Montados and Dehesas for high nature value: an interdisciplinary pathway. Agrofor. Syst. 90, 1–6. https://doi.org/10.1007/s10457-016-9900-8.

Frampton, W.J., Dash, J., Watmough, G., Milton, E.J., 2013. Evaluating the capabilities of Sentinel-2 for quantitative estimation of biophysical variables in vegetation. ISPRS J. Photogramm. Remote Sens. 82, 83–92. https://doi.org/10.1016/j.isprsjprs.2013.04.007.

Frenich, A.G., Jouan-Rimbaud, D., Massart, D.L., Kuttatharmmakul, S., Galera, M.M., Vidal, J.M., 1995. Wavelength selection method for multicomponent spectrophotometric determinations using partial least squares. Analyst 120, 2787–2792.

Friedl, H., Stampfer, E., 2002. Jackknife resampling. Encyclopedia of Environmetrics. vol. 2. Wiley, pp. 1089–1098.

Gao, J., 2006. Quantification of grassland properties: How it can benefit from geoinformatic technologies? Int. J. Remote Sens. 27, 1351–1365. https://doi.org/10.1080/01431160500474357.

García-Ciudad, A., García-Criado, B., Pérez-Corona, M.E., De Aldana, B.R.V., Ruano-Ramos, A.M., 1993. Application of near-infrared reflectance spectroscopy to chemical analysis of heterogeneous and botanically complex grassland samples. J. Sci. Food Agric. 63, 419–426. https://doi.org/10.1002/jsfa.2740630407.

Gascon, F., Bouzinac, C., Thépaut, O., Jung, M., Francesconi, B., Louis, J., ... Fernandez, V., 2017. Copernicus Sentinel-2A calibration and products validation status. Remote Sens. 9, 584. https://doi.org/10.3390/rs9060584.

Giannakopoulos, C., Le Sager, P., Bindi, M., Moriondo, M., Kostopoulou, E., Goodess, C.M., 2009. Climatic changes and associated impacts in the Mediterranean resulting from a 2 °C global warming. Glob. Planet. Chang. 68, 209–224. https://doi.org/10.1016/j.gloplacha.2009.06.001.

Giorgi, F., Lionello, P., 2008. Climate change projections for the Mediterranean region. Glob. Planet. Chang. 63, 90–104. https://doi.org/10.1016/j.gloplacha.2007.09.005.

Global Climate Monitor, 2020. Global Climate Monitor. https://www.globalclimatemonitor.org (accessed 11November 2020).

Gómez-Giráldez, P.J., Aguilar, C., Caño, A.B., García-Moreno, A., González-Dugo, M.P., 2019. Remote sensing estimation of net primary production as monitoring indicator of holm oak savanna management. Ecol. Indic. 106, 105526. https://doi.org/10.1016/j.ecolind.2019.105526.

Gómez-Giráldez, P.J., Pérez-Palazón, M.J., Polo, M.J., González-Dugo, M.P., 2020. Monitoring grass phenology and hydrological dynamics of an oak-grass savanna ecosystem using sentinel-2 and terrestrial photography. Remote Sens. 12, 600. https://doi.org/10.3390/rs12040600.

Goodhue, D.L., Lewis, W., Thompson, R., 2012. Does PLS have advantages for small sample size or non-normal data? MIS Q. 36, 981–1001. https://doi.org/10.2307/41703490.

Gorelick, N., Hancher, M., Dixon, M., Ilyushchenko, S., Thau, D., Moore, R., 2017. Google Earth Engine: planetary-scale geospatial analysis for everyone. Remote Sens. Environ. 202, 18–27. https://doi.org/10.1016/j.rse.2017.06.031.

Habitats Directive, 1992. Council Directive 92/43/EEC of 21 May 1992 on the conservation of natural habitats and of wild fauna and flora. (Brussels, Belgium). https://ec.europa.eu/environment/nature/legislation/habitatsdirective/index_en.htm. (Accessed 2 April 2021).

Harlio, A., Kuussaari, M., Heikkinen, R.K., Arponen, A., 2019. Incorporating landscape heterogeneity into multi-objective spatial planning improves biodiversity conservation of semi-natural grasslands. J. Nat. Conserv. 49, 37–44. https://doi.org/10.1016/j.jnc.2019.01.003.

Igne, B., Reeves, J.B., McCarty, G., Hively, W.D., Lundc, E., Hurburgh, C.R., 2010. Evaluation of spectral pretreatments, partial least squares, least squares support vector machines and locally weighted regression for quantitative spectroscopic analysis of soils. J. Near Infrared Spectrosc. 18, 167–176. https://doi.org/10.1255/jnirs.883.

Jacquemoud, S., Verdebout, J., Schmuck, G., Andreoli, G., Hosgood, B., 1995. Investigation of leaf biochemistry by statistics. Remote Sens. Environ. 54, 189–197. https://doi.org/10.1016/0034-4257(95)00174-3.

Jacquemoud, Stéphane, Verhoef, W., Baret, F., Bacour, C., Zarco-Tejada, P.J., Asner, G.P., ... Ustin, S.L., 2009. PROSPECT + SAIL models: a review of use for vegetation characterization. Remote Sens. Environ. 113, 56–S66. https://doi.org/10.1016/j.rse.2008.01.026.

Jouan-Rimbaud, D., Massart, D.L., Saby, C.A., Puel, C., 1998. Determination of the representativity between two multidimensional data sets by a comparison of their structure. Chemom. Intell. Lab. Syst. 40, 129–144. https://doi.org/10.1016/S0169-7439(98)00005-7.

Justice, C.O., Townshend, J.G., 1981. Integrating ground data with remote sensing. In: Townshend, J.G. (Ed.), Terrain Analysis and Remote Sensing. Allen and Unwin, London, pp. 38–58.

Kassambara, A., Mundt, F., 2017. Package 'factoextra'. Extract and Visualize the Results of Multivariate Data Analyses. 76.

Kattenborn, T., Fassnacht, F.E., Schmidtlein, S., 2019. Differentiating plant functional types using reflectance: which traits make the difference? Remote. Sens. Ecol. Conserv. 5, 5–19. https://doi.org/10.1002/rse2.86.

Kawamura, K., Watanabe, N., Sakanoue, S., Inoue, Y., 2008. Estimating forage biomass and quality in a mixed sown pasture based on partial least squares regression with waveband selection. Grassl. Sci. 54, 131–145. https://doi.org/10.1111/j.1744-697x.2008.00116.x.

Knadel, M., Deng, F., Thomsen, A., Greve, M.H., 2012. Development of a Danish national Vis–NIR soil spectral library for soil organic carbon determination. In: Minasny, B., Malone, B.P., McBratney, A.B. (Eds.), Digital Soil Assessments and Beyond: Proceedings of the 5th Global Workshop on Digital Soil Mapping 2012. CRC Press, Sydney, Australia, pp. 403–408.

Kodinariya, T.M., Makwana, P.R., 2013. Review on determining number of Cluster in K-Means Clustering. Int. J. Adv. Res. Comput. Sci. Manag. Stud. 1, 2321–7782.

Kokaly, R.F., 2001. Investigating a physical basis for spectroscopic estimates of leaf nitrogen concentration. Remote Sens. Environ. 75, 153–161. https://doi.org/10.1016/S0034-4257(00)00163-2.

Kucheryavskiy, S., 2018. Analysis of NIR spectroscopic data using decision trees and their ensembles. J. Anal. Test 2, 274–289. https://doi.org/10.1007/s41664-018-0078-0.

Kucheryavskiy, A.S., 2019. Package 'mdatools.'.

Kucheryavskiy, S., 2020a. Getting started with mdatools for R. https://mdatools.com/docs/distances-and-outlier-detection.html. (Accessed 2 February 2020).

Kucheryavskiy, S., 2020b. mdatools – R package for chemometrics. Chemom. Intell. Lab. Syst. 198, 103937. https://doi.org/10.1016/j.chemolab.2020.103937.

Li, B., Morris, J., Martin, E.B., 2002. Model selection for partial least squares regression. Chemom. Intell. Lab. Syst. 64, 79–89. https://doi.org/10.1016/S0169-7439(02)00051-5.

Linea, 2020. Localizador de Información espacial de Andalucía. Available at: http://www.juntadeandalucia.es/institutodeestadisticaycartografia/lineav2/web/. (Accessed 9 March 2020).

Liu, Y., Shi, Z., Zhang, G., Chen, Y., Li, S., Hong, Y., ... Liu, Y., 2018. Application of spectrally derived soil type as ancillary data to improve the estimation of soil organic carbon by using the Chinese Soil Vis-NIR spectral library. Remote Sens. 10. https://doi.org/10.3390/rs10111747.

Lobos, I., Gou, P., Hube, S., Saldaña, R., Alfaro, M., 2013. Evaluation of potential nirs to predict pastures nutritive value. J. Soil Sci. Plant Nutr. 13, 463–468. https://doi.org/10.4067/S0718-95162013005000036.

López-Carrasco, C., López-Sánchez, A., San Miguel, A., Roig, S., 2015. The effect of tree cover on the biomass and diversity of the herbaceous layer in a Mediterranean dehesa. Grass Forage Sci. 70, 639–650. https://doi.org/10.1111/gfs.12161.

Lu, B., He, Y., 2017. Species classification using Unmanned Aerial Vehicle (UAV)-acquired high spatial resolution imagery in a heterogeneous grassland. ISPRS J. Photogramm. Remote Sens. 128, 73–85. https://doi.org/10.1016/j.isprsjprs.2017.03.011.

Lugassi, R., Zaady, E., Goldshleger, N., Shoshany, M., Chudnovsky, A., 2019. Spatial and temporal monitoring of pasture ecological quality: Sentinel-2-based estimation of crude protein and neutral detergent fiber contents. Remote Sens. 11, 799. https://doi.org/10.3390/rs11070799.

Ma, Z., Liu, H., Mi, Z., Zhang, Z., Wang, Y., Xu, W., ... He, J.S., 2017. Climate warming reduces the temporal stability of plant community biomass production. Nat. Commun. 8, 1–7. https://doi.org/10.1038/ncomms15378.

Mansour, K., Mutanga, O., Terry, E., 2012. Remote sensing based indicators of vegetation species for assessing rangeland degradation: opportunities and challenges. Afr. J. Agric. Res. 7, 3261–3270. https://doi.org/10.5897/ajarx11.2316.

Marañón, T., 1991. Diversidad en comunidades de pastomediterráneo: modelos y mecanismos de coexistencia. Ecología 5, 149–157.

Martens, H., Martens, M., 2000. Modified Jack-knife estimation of parameter uncertainty in bilinear modelling by partial least squares regression (PLSR). Food Qual. Prefer. 11, 5–16. https://doi.org/10.1016/S0950-3293(99)00039-7.

Martens, H., Naes, T., 1992. MultiVariate Calibration. John Wiley and Sons, New York.

Morellos, A., Pantazi, X.E., Moshou, D., Alexandridis, T., Whetton, R., Tziotzios, G., ... Mouazen, A.M., 2016. Machine learning based prediction of soil total nitrogen, organic carbon and moisture content by using VIS-NIR spectroscopy. Biosyst. Eng. 152, 104–116. https://doi.org/10.1016/j.biosystemseng.2016.04.018.

Moreno, G., Pulido, F., 2009. The functioning, management and persistence of dehesas. Agroforestry in Europe. Vol. 6. Springer, Dordrecht, pp. 127–160. https://doi.org/10.1007/978-1-4020-8272-6.

Mueller-Wilm, U., Devignot, O., Pessiot, L., 2017. S2 MPC Sen2Cor Configuration and UserManual (No. S2-PDGS-MPC-L2A-SUM-V2.4). ESA.

Mutanga, O., Skidmore, A.K., Prins, H.H.T., 2004. Predicting in situ pasture quality in the Kruger National Park, South Africa, using continuum-removed absorption features. Remote Sens. Environ. 89, 393–408. https://doi.org/10.1016/j.rse.2003.11.001.

Mutanga, O., Adam, E., Adjorlolo, C., Abdel-Rahman, E.M., 2015. Evaluating the robustness of models developed from field spectral data in predicting African grass foliar nitrogen concentration using WorldView-2 image as an independent test dataset. Int. J. Appl. Earth Obs. Geoinf. 34, 178–187. https://doi.org/10.1016/j.jag.2014.08.008.

Myers, N., Mittermeier, R.A., Mittermeier, C.G., Da Fonseca, G.A., Kent, J., 2000. Biodiversity hotspots for conservation priorities. Nature 403, 853–858. https://doi.org/10.1038/35002501.

Nieke, J., Rast, M., 2018. Towards the Copernicus Hyperspectral Imaging Mission For The Environment (CHIME). IGARSS 2018–2018 IEEE International Geoscience and Remote Sensing Symposium. IEEE, Valencia, Spain, pp. 157–159.

Norris, K.H., Barnes, R.F., 1976. Infrared reflectance analysis of nutritive value of feedstuffs. Proceedings' of First International Symposium on Feed Composition, Animal Nutrient Requirements, and Computerization. Utah State University, Logan, UT.

Olea, L., San Miguel-Ayanz, A., 2006. The Spanish dehesa. A traditional Mediterranean silvopastoral system linking production and nature conservation. In: Lloveras, J., González-Rodríguez, A., Vázquez-Yáñez, O., Piñeiro, J., Santamaría, L.O., Poblaciones, M.J. (Eds.), Sustainable Grassland Productivity, Grassland Science in Europe, vol. 11. Sociedad Española para el Estudio de los Pastos, Badajoz, Spain, pp. 3–13.

Paracchini, M.L., Petersen, J.E., Hoogeveen, Y., Bamps, C., Burfield, I., van Swaay, C., 2008. High nature value farmland in Europe – an estimate of the distribution patterns on the basis of land cover and biodiversity data. JRC Scientific and Technical Report EUR 23480 EN (87 pp).

Parrini, S., Acciaioli, A., Crovetti, A., Bozzi, R., 2018. Use of FT-NIRS for determination of chemical components and nutritional value of natural pasture. Ital. J. Anim. Sci. 17, 87–91. https://doi.org/10.1080/1828051X.2017.1345659.

Pellissier, P.A., Ollinger, S.V., Lepine, L.C., Palace, M.W., McDowell, W.H., 2015. Remote sensing of foliar nitrogen in cultivated grasslands of human dominated landscapes. Remote Sens. Environ. 167, 88–97. https://doi.org/10.1016/j.rse.2015.06.009.

Perez Corona, M.E., Vazquez de Aldana, B.R., Garci, B., Garci, A., 1998. Variations in nutritional quality and biomass production of semiarid grasslands. Rangel. Ecol. Manag. 51, 570–576.

Pérez-Ramos, I.M., Cambrollé, J., Hidalgo-Galvez, M.D., Matías, L., Montero-Ramírez, A., Santolaya, S., Godoy, Ó., 2020. Phenological responses to climate change in communities of plants species with contrasting functional strategies. Environ. Exp. Bot. 170, 103852. https://doi.org/10.1016/j.envexpbot.2019.103852.

Plieninger, T., Wlbrand, C., 2001. Land use, biodiversity conservation, and rural development in the dehesas of Cuatro Lugares, Spain. Agrofor. Syst. 51, 23–34. https://doi.org/10.1023/A:1006462104555.

Porqueddu, C., Ates, S., Louhaichi, M., Kyriazopoulos, A.P., Moreno, G., del Pozo, A., ... Nichols, P.G.H., 2016. Grasslands in "Old World" and "New World" Mediterranean-climate zones: past trends, current status and future research priorities. Grass Forage Sci. 71, 1–35. https://doi.org/10.1111/gfs.12212.

Porqueddu, C., Melis, R.A.M., Franca, A., Sanna, F., Hadjigeorgiou, I., Casasús Pueyo, I., 2017. The role of grasslands in the less favoured areas of Mediterranean Europe. 19th European Grassland Federation Symposium: Grassland Resources for Extensive Farming Systems in Marginal Lands: Major Drivers and Future Scenarios, Alghero, Sardinia (Italy), 7–10 may 2017.

Pullanagari, R.R., Yule, I.J., Tuohy, M.P., Hedley, M.J., Dynes, R.A., King, W.M., 2012. In-field hyperspectral proximal sensing for estimating quality parameters of mixed pasture. Precis. Agric. 13, 351–369. https://doi.org/10.1007/s11119-011-9251-4.

Pullanagari, R.R., Dynes, R.A., King, W.M., Yule, I.J., Thulin, S., Knox, N.M., Ramoelo, A., 2013. Remote sensing of pasture quality. In: Michalk, D.L., Millar, G.D., Badgery, W.B., Broadfoot, K.M. (Eds.), Revitalising Grasslands to Sustain our Communities—Proceedings of the 22nd International Grassland Congress. NSW. Department of Primary Industry, Orange, pp. 633–638.

Pullanagari, R.R., Dehghan-Shoar, M., Yule, I.J., Bhatia, N., 2021. Field spectroscopy of canopy nitrogen concentration in temperate grasslands using a convolutional neural network. Remote Sens. Environ. 257, 112353. https://doi.org/10.1016/j.rse.2021.112353.

Punalekar, S.M., Verhoef, A., Quaife, T.L., Humphries, D., Bermingham, L., Reynolds, C.K., 2018. Application of Sentinel-2A data for pasture biomass monitoring using a

physically based radiative transfer model. Remote Sens. Environ. 218, 207–220. https://doi.org/10.1016/j.rse.2018.09.028.
R Development Core Team, 2019. R: A language and environment for statistical computing. R Foundation for Statistical Computing, Vienna, Austria URL. https://www.R-project.org/.
Raab, C., Riesch, F., Tonn, B., Barrett, B., Meißner, M., Balkenhol, N., Isselstein, J., 2020. Target-oriented habitat and wildlife management: estimating forage quantity and quality of semi-natural grasslands with Sentinel-1 and Sentinel-2 data. Remote. Sens. Ecol. Conserv. 6, 381–398. https://doi.org/10.1002/rse2.149.
Ramoelo, A., Cho, M.A., 2018. Explaining leaf nitrogen distribution in a semi-arid environment predicted on sentinel-2 imagery using a field spectroscopy derived models. Remote Sens. 10, 269. https://doi.org/10.3390/rs10020269.
Ramoelo, A., Skidmore, A.K., Schlerf, M., Mathieu, R., Heitkönig, I.M.A., 2011. Water-removed spectra increase the retrieval accuracy when estimating savanna grass nitrogen and phosphorus concentrations. ISPRS J. Photogramm. Remote Sens. 66, 408–417. https://doi.org/10.1016/j.isprsjprs.2011.01.008.
Ramoelo, A., Cho, M., Mathieu, R., Skidmore, A.K., 2015. Potential of Sentinel-2 spectral configuration to assess rangeland quality. J. Appl. Remote. Sens. 9, 094096. https://doi.org/10.1117/1.jrs.9.094096.
Rast, M., Ananasso, C., Bach, H., Ben-Dor, E., Chabrillat, S., Colombo, R., ... Strobl, P., 2019. Copernicus hyperspectral imaging mission for the environment: mission requirements document (ESA-EOPSM-CHIM-MRD-3216). Earth and Mission Science Division, European Space Agency http://esamultimedia.esa.int/docs/EarthObservation/Copernicus_CHIME_MRD_v2.1_Issued20190723.pdf. (Accessed 14 September 2020).
REDIAM, 2020. WMS Distribución de las formaciones adehesadas en Andalucía. http://www.juntadeandalucia.es/medioambiente/mapwms/REDIAM_distribucion_formaciones_adehesadas. (Accessed 13 May 2020).
Ripple, W.J., 1986. Spectral reflectance relationships to leaf water stress. Photogramm. Eng. Remote. Sens. 52, 1669–1675.
Rodionova, O.Y., Pomerantsev, A.L., 2020. Detection of outliers in projection-based modeling. Anal. Chem. 92, 2656–2664 (research-article). https://doi.org/10.1021/acs.analchem.9b04611.
Rodwell, J.S., Schaminée, J.H.J., Mucina, L., Pignatti, S., Dring, J., Moss, D., 2002. The diversity of European vegetation. An overview of phytosociological alliances and their relationships to EUNIS habitats. National Reference Centre for Agriculture, Nature and Fisheries, Wageningen, NL.
Santos-Rufo, A., Mesas-Carrascosa, F.J., García-Ferrer, A., Meroño-Larriva, J.E., 2020. Wavelength selection method based on partial least square from hyperspectral unmanned aerial vehicle orthomosaic of irrigated olive orchards. Remote Sens. 12, 3426. https://doi.org/10.3390/rs12203426.
Serrano, J., Shahidian, S., da Silva, J.M., 2018. Monitoring seasonal Pasture Quality Degradation in the Mediterranean montado ecosystem: proximal versus remote sensing. Water 10, 1422. https://doi.org/10.3390/w10101422.
Shenk, J.S., Westerhaus, M.O., 1996. Calibration the ISI way. Near Infrared Spectroscopy: the Future Waves. NIR Publications, Chichester, pp. 198–202.
Shepherd, K.D., Walsh, M.G., 2002. Development of reflectance spectral libraries for characterization of soil properties. Soil Sci. Soc. Am. J. 66, 988–998. https://doi.org/10.2136/sssaj2002.9880.
Simoncini, R., Ring, I., Sandström, C., Albert, C., Kasymov, U., Arlettaz, R., 2019. Constraints and opportunities for mainstreaming biodiversity and ecosystem services in the EU's Common Agricultural Policy: insights from the IPBES assessment for Europe and Central Asia. Land Use Policy 88, 104099. https://doi.org/10.1016/j.landusepol.2019.104099.
Starks, P.J., Zhao, D., Phillips, W.A., Coleman, S.W., 2006. Development of canopy reflectance algorithms for real-time prediction of bermudagrass pasture biomass and nutritive values. Crop Sci. 46, 927–934. https://doi.org/10.2135/cropsci2005.0258.
Stevens, A., Ramirez-Lopez, L., 2014. An introduction to the prospectr package. R Package Vignette. R Package Version 0.1, 3.
Stumpf, F., Schneider, M.K., Keller, A., Mayr, A., Rentschler, T., Meuli, R.G., ... Liebisch, F., 2020. Spatial monitoring of grassland management using multi-temporal satellite imagery. Ecol. Indic. 113, 106201. https://doi.org/10.1016/j.ecolind.2020.106201.
Tong, A., He, Y., 2017. Estimating and mapping chlorophyll content for a heterogeneous grassland: Comparing prediction power of a suite of vegetation indices across scales between years. ISPRS J. Photogramm. Remote Sens. 126, 146–167. https://doi.org/10.1016/j.isprsjprs.2017.02.010.
Ustin, S.L., Gitelson, A.A., Jacquemoud, S., Schaepman, M., Asner, G.P., Gamon, J.A., Zarco-Tejada, P., 2009. Retrieval of foliar information about plant pigment systems from high resolution spectroscopy. Remote Sens. Environ. 113, 67–S77. https://doi.org/10.1016/j.rse.2008.10.019.
Valderrama, P., Braga, J.W.B., Poppi, R.J., 2007. Variable selection, outlier detection, and figures of merit estimation in a partial least-squares regression multivariate calibration model. A case study for the determination of quality parameters in the alcohol industry by near-infrared spectroscopy. J. Agric. Food Chem. 55, 8331–8338. https://doi.org/10.1021/jf071538s.
Vázquez-De-Aldana, B.R., García-Ciudad, A., García-Criado, B., 2008. Interannual variations of above-ground biomass and nutritional quality of Mediterranean grasslands in Western Spain over a 20-year period. Aust. J. Agric. Res. 59, 769–779. https://doi.org/10.1071/AR07359.
Viscarra Rossel, R.A., McGlynn, R.N., McBratney, A.B., 2006. Determining the composition of mineral-organic mixes using UV–vis-NIR diffuse reflectance spectroscopy. Geoderma 137, 70–82. https://doi.org/10.1016/j.geoderma.2006.07.004.
Wachendorf, M., Fricke, T., Möckel, T., 2018. Remote sensing as a tool to assess botanical composition, structure, quantity and quality of temperate grasslands. Grass Forage Sci. 73, 1–14. https://doi.org/10.1111/gfs.12312.
Wang, Y., Liu, Q., Hou, H.D., Rho, S., Gupta, B., Mu, Y.X., Shen, W.Z., 2018. Big data driven outlier detection for soybean straw near infrared spectroscopy. J. Comput. Sci. 26, 178–189. https://doi.org/10.1016/j.jocs.2017.06.008.
Williams, P.C., Sobering, D., 1996. How do we do it: a brief summary of the methods we use in developing near infrared calibrations. In: Davies, A.M.C., Williams, P.C. (Eds.), Near Infrared Spectroscopy: The Future Waves. NIR Publications, Hichester, West Sussex, UK, pp. 185–188.
Wold, H., 1966. Nonlinear estimation by iterative least square procedures. Research Papers in Statistics. Wiley, New York, pp. 411–444.
Wold, S., 1978. Cross-validatory estimation of the number of components in factor and principal components models. Technometrics 20, 397–405. https://doi.org/10.1080/00401706.1978.10489693.
Wold, S., Sjöström, M., Eriksson, L., 2001. PLS-regression: a basic tool of chemometrics. Chemom. Intell. Lab. Syst. 58, 109–130. https://doi.org/10.1016/S0169-7439(01)00155-1.
Wolfert, S., Ge, L., Verdouw, C., Bogaardt, M.J., 2017. Big data in smart farming – a review. Agric. Syst. 153, 69–80. https://doi.org/10.1016/j.agsy.2017.01.023.
Xu, L., Li, J., Brenning, A., 2014. A comparative study of different classification techniques for marine oil spill identification using RADARSAT-1 imagery. Remote Sens. Environ. 141, 14–23. https://doi.org/10.1016/j.rse.2013.10.012.
Xu, S., Zhao, Y., Wang, M., Shi, X., 2018. Comparison of multivariate methods for estimating selected soil properties from intact soil cores of paddy fields by Vis–NIR spectroscopy. Geoderma 310, 29–43. https://doi.org/10.1016/j.geoderma.2017.09.013.
Yue, J., Tian, Q., Dong, X., Xu, N., 2020. Using broadband crop residue angle index to estimate the fractional cover of vegetation, crop residue, and bare soil in cropland systems. Remote Sens. Environ. 237, 111538. https://doi.org/10.1016/j.rse.2019.111538.
Zeng, L., Chen, C., 2018. Using remote sensing to estimate forage biomass and nutrient contents at different growth stages. Biomass Bioenergy 115, 74–81. https://doi.org/10.1016/j.biombioe.2018.04.016.
Zhou, Z., Morel, J., Parsons, D., Kucheryavskiy, S.V., Gustavsson, A.M., 2019. Estimation of yield and quality of legume and grass mixtures using partial least squares and support vector machine analysis of spectral data. Comput. Electron. Agric. 162, 246–253. https://doi.org/10.1016/j.compag.2019.03.038.